Validation of a novel immersive virtual reality set-up with responses of wild-caught freely moving coral reef fish

Manuel Vidal, Suzanne Mills, Emma Gairin, Frédéric Bertucci, David Lecchini

Animal Behaviour 206 (2023) 99–123

Contents lists available at ScienceDirect

Animal Behaviour

journal homepage: www.elsevier.com/locate/anbehav

Methods

Validation of a novel immersive virtual reality set-up with responses of wild-caught freely moving coral reef fish

Manuel Vidal [a, *], Suzanne C. Mills [b, c], Emma Gairin [d], Frédéric Bertucci [b, e], David Lecchini [b, c]

[a] Institut de Neurosciences de la Timone, UMR 7289, Aix-Marseille Université, CNRS, Marseille, France
[b] PSL Université Paris, EPHE-UPVD-CNRS, UAR3278 CRIOBE, Moorea, French Polynesia
[c] Laboratoire d'Excellence 'CORAIL', France
[d] Marine Eco-Evo-Devo Unit, Okinawa Institute of Science and Technology, Okinawa, Japan
[e] Marbec, CNRS-IRD-IFREMER-INRAE-University of Montpellier, Sète, France

ARTICLE INFO

Article history:
Received 3 May 2023
Initial acceptance 16 May 2023
Final acceptance 21 July 2023
Available online 3 November 2023
MS. number: 23-00223R

Keywords:
conspecific
habitat
postlarval
predator
proof of concept
recruitment
reef fish
virtual reality
visual recognition

Virtual reality (VR) enables standardized stimuli to provoke behavioural responses in animals; however, in fish studies VR has been limited to either basic virtual simulation projected below the bowl for freely swimming individuals or a simple virtual arena rendered over a large field of view for head-restrained individuals. We developed a novel immersive VR set-up with real-time rendering of animated 3D scenarios, validated in a proof-of-concept study on the behaviour of coral reef postlarval fish. Fish use a variety of cues to select a habitat during the recruitment stage, and to recognize conspecifics and predators, but which visual cues are used remains unknown. We measured behavioural responses of groups of five convict postlarval surgeonfish, *Acanthurus triostegus*, to simulations of habitats, static or moving shoals of conspecifics, predators and nonaggressive heterospecifics. Postlarval fish were consistently attracted to virtual corals and conspecifics presented statically, but repulsed by their predators (bluefin jacks, *Caranx melampygus*). When simulated shoals repeatedly passed nearby, they were again attracted by conspecifics, showing a tendency to follow the shoal, whereas they moved repeatedly to the back of the passing predator shoal. They also discriminated between species of similar sizes: they were attracted more to conspecifics than butterflyfish, *Forcipiger longirostris*, and repulsed more by predators than parrotfish, *Scarus psittacus*. The quality of visual simulations was high enough to identify visual cues (size, body shape, colour pattern) used by postlarval fish in species recognition. Despite a tracking technology limited to fish 2D positions in the aquarium, preventing the real-time updating of the rendered viewpoint, we could show that VR and modern tracking technologies offer new possibilities to investigate fish behaviour through the quantitative analysis of their physical reactions to highly controlled scenarios.

Animal behaviours, such as foraging, habitat choice, predator avoidance, social behaviour and mate choice, are studied for multiple reasons including to understand how they have been shaped by natural selection or how they are impacted by internal and external stimuli. Animal behavioural studies face two challenges: one is related to the subject's own understanding of the task to be performed and the other is linked to measuring its response (Drew, 2019). One way to solve the first challenge is to use a task that requires a natural reaction to a stimulus presented in an ecological context, and for which the understanding is implicit. Conventional experimental approaches used live stimulus animals or environments, but they suffered from a lack of control and standardization as neither the behaviour of stimulus animals nor the local environment can be completely controlled. For instance, testing behavioural dominance in response to an opponent requires trials with multiple opponents of known dominance and applying a correction factor (Alatalo et al., 1991; Mills et al., 2007). Furthermore, experiments with live stimulus animals often require long methodological preparation, which limits the number of possible manipulations (Neri, 2012). As a result, stimuli have been artificially designed to provide repeatable behavioural

* Corresponding author.
E-mail address: manuel.vidal@univ-amu.fr (M. Vidal).

https://doi.org/10.1016/j.anbehav.2023.09.013

observations (Carmichael, 1952) and have evolved from simple pictures and physical models to virtual reality (VR) that enables standardized manipulations of stimulus behaviours or environments. The second challenge, response measurement, has been solved using video-based tracking systems of freely moving focal animals, which assumes that the behavioural response lies in the kinematics of the animal, for example position, orientation, speed, spatial dispersion. Therefore, VR provides a good methodological compromise between a perfectly controlled but not ecologically valid stimulus and a realistic natural situation with little to no parameter control. Although VR simulators have been widely used over the last 25 years to elucidate the perceptual, sensorimotor and cognitive mechanisms underlying human spatial orientation in the environment (e.g. Mossio et al., 2008; Tarr & Warren, 2002; Vidal & Bülthoff, 2009; Vidal et al., 2004, 2009), only recently have they been adapted to investigate animal behaviour, ranging from mice, *Mus musculus*, to fruit flies, *Drosophila* spp., and zebrafish, *Danio rerio* (Harvey et al., 2009; Stowers et al., 2017; for a discussion, see Drew, 2019).

The first studies of fish visual behaviour that used prerecorded video stimuli in mating preference tasks date from the end of the nineties, with either manipulated real videos of fish (Rosenthal & Evans, 1998) or synthetically generated videos of 3D animated fish (Künzler & Bakker, 1998). Ten years later, the same team showed that computer animations of artificial fish allowed them to manipulate movement, body shape and skin colour to investigate preferences in the cichlid *Pelvicachromis taeniatus* (Baldauf et al., 2009). The survival potential of prey group formation and movement was measured through the response of real predatory bluegill sunfish, *Lepomis macrochirus*, to virtual prey projections (Ioannou et al., 2012). Both experiments used one or two screen monitors to display the virtual images. Since then, technology has greatly improved, and VR has led to considerable advances in the understanding of the neural bases of zebrafish visual behaviour (Dunn et al., 2016; Portugues & Engert, 2009), shoaling behaviour and social interactions (Harpaz et al., 2021; Huang et al., 2020; Larsch & Baier, 2018), as well as decision making (Barker & Baier, 2015). However, the use of VR to study fish behaviour has been restricted to zebrafish larvae, either moving freely in a bowl and responding to basic virtual simulation projected below such as moving dark disks, a checkerboard or grass bottom, coupled with infrared 3D tracking (Stowers et al., 2017), or with head-restrained zebrafish responding to conspecifics in a simple virtual arena covering 180° of the visual field and rotating based on tail movements (Huang et al., 2020). Therefore, modern VR technology including realistic rendering and immersion in a large 3D volume has not been adapted to fish studies yet, despite the limitless number of findings that can be generated in terms of quantitative animal behaviour and their ecological implications. Here, we carried out a proof-of-concept study on a new set-up for freely moving fish within an aquarium with an immersive full-field rendering of virtual scenes using projections not only from below, but also on all five sides (except the top). We propose that our VR set-up has considerable future potential for all types of behavioural studies on fish species at any stage of their life cycle. We tested our methodology on the behaviour of postlarval coral reef fish exposed to multiple scenarios during their recruitment.

In all marine environments, one of the main mysteries of fish ecology is how larvae recruit onto the relatively rare patches of coastal habitats (for a review, see Barth et al., 2015; Doherty, 2002). The life cycle of most reef fish species starts with a planktonic larval phase, lasting several weeks, followed by recruitment and a sedentary reef phase for juveniles and adults (Leis & McCormick, 2002). At the end of the pelagic phase, this recruitment relies on the detection of a suitable habitat which will facilitate larval survival and growth (Doherty, 2002; Lecchini & Galzin, 2003). Simultaneous to that choice, species-specific changes in morphology and physiology, metamorphosis, occur. These changes are linked to ecological shifts with modifications not only of diet and diel activity period (Besson et al., 2017; Holzer et al., 2017; McCormick et al., 2002) but also of the sensory systems (Lecchini et al., 2005; Tettamanti et al., 2019). Many studies have highlighted the role of sensory and swimming mechanisms in larval habitat selection, most focusing on the role of chemical (e.g. Atema et al., 2002; Coppock et al., 2013; Lecchini et al., 2013; Vail & McCormick, 2011) and acoustic cues (e.g. Holles et al., 2013; Montgomery et al., 2006; Parmentier et al., 2015; Tolimieri et al., 2004). However, vision is a well-developed sense in coral reef fish larvae (Myrberg & Fuiman, 2002), effective to up to 10 m for *Plectropomus leopardus* postlarval fish at recruitment (Leis & Carson-Ewart, 1999). Once larvae are close to a reef, visual cues of conspecifics become important in the recruitment process (Barth et al., 2015; Booth, 1992). However, only a few studies have identified the visual parameters used by larvae to recognize conspecifics or predators (e.g. Booth, 1992; Huijbers et al., 2012; Lecchini et al., 2014; Leis & Carson-Ewart, 1999). To test how postlarval fish (i.e. larvae having recruited onto a habitat, with metamorphosis still ongoing; see Besson et al., 2020) interpret a range of sensory cues, behavioural experiments can reproduce and control a large variety of combinations of visual cues (Barth et al., 2015). VR is potentially an excellent method to test such behaviours as visual factors such as size, colour patterns and the behaviour of other individuals can be tightly controlled (Brookes et al., 2020; Stowers et al., 2017). In this study, we experimentally validated a new and fully immersive VR set-up for fish by testing several presentation scenarios, named trials, in three experiments on postlarval fish during recruitment.

We used an innovative immersive VR set-up to understand how postlarval convict surgeonfish, *Acanthurus triostegus*, visually recognize a suitable habitat, adult conspecifics and one of their predators (bluefin jacks, *Caranx melampygus*). Our first objective was to experimentally validate the use of simulated 3D models of fishes in a VR set-up by confirming that they are realistic enough to cause natural reactions in postlarval fish. Three main experiments were carried out to identify the visual cues used by surgeonfish postlarvae to recognize adult conspecifics and a predator. Trials included the presentation of virtual habitats (healthy or bleached coral reefs) or virtual monospecific fish shoals of conspecifics or predators. The virtual fish projected were either static (moving in place, experiments 1 and 2) or dynamic (swimming past on one side of the aquarium, experiments 2 and 3). In these experiments we aimed to virtually reproduce previous studies in which the reaction to either static fish in the corners of the aquarium (Katzir, 1981) or to real fish swimming in a separate adjacent aquarium (Roux et al., 2016) had been studied. We also tested postlarval behavioural responses to two virtual fish shoals swimming past on either side of the aquarium, each with different species, inducing a forced choice (experiment 3). This experiment was also designed to test whether postlarvae can discriminate between the size and species of virtual fish, that is, whether postlarval fish consider larger virtual fish as threats irrespective of species. The advantage of our virtual presentation compared to using live stimuli is that we were able to measure postlarval fish behaviour rapidly in response to different trials. Our second objective was to validate the automation of postlarval fish position tracking within the test aquarium at high temporal resolution, enabling detailed characterization of their behavioural responses to each scenario.

THE IMMERSIVE VR SET-UP

The experimental set-up was composed of three connected modules: the focal aquarium in which postlarvae could swim freely suspended inside the test aquarium, the rendering module that projected the interactive 3D virtual environments depicting a subaquatic natural scene with fishes and corals, and the tracking module which recorded postlarval behaviour in real time. The software was developed in the laboratory and the hardware was assembled by Immersion (https://www.immersion.com).

Test and Focal Aquaria

The test aquarium was a rectangular prism made of 10 mm thick Plexiglas plates, with a 50 × 50 cm square bottom and 35 cm high lateral sides. The external faces of the bottom and lateral sides were covered by a translucent, but not transparent, rear projection film, so that postlarval fish inside the aquarium could not see the room surrounding the set-up, except for the ceiling. The aquarium was filled with 78 litres of sea water so that the water surface was aligned with the upper limit of the video projection. The entire set-up was mounted on a structure made of 4 cm squared-section aluminium bars (Fig. 1a). A smaller focal aquarium (dimensions 20 × 20 × 20 cm) in which the postlarvae were placed was attached to the structure using chains and positioned inside the test aquarium (Fig. 1b). This smaller focal aquarium limited postlarval movement maintaining them within the range where geometrical projection distortion and image corrections were minimal and would not affect postlarval behaviour (see Video-based tracking section).

Virtual Scene Rendering

Five video projectors ensured an immersive full field rendering of the virtual scenes on five sides of the test aquarium (Optoma ML1050ST+, running at 60 Hz with a resolution of 1280 × 800 for the side views and 800 × 800 for the bottom view). The visible range of postlarval surgeonfish likely falls within the human visible range, enabling the use of these video projectors for visual stimulation (Losey et al., 2003). The baseline 3D virtual environment, which was always projected onto all five aquarium sides, consisted of a sandy bottom at 2 m, with simulated surface ripples and caustics projected on the ground. The virtual viewpoint (position of rendering cameras), which defines the physical-to-virtual relationship, was placed at a depth of 0.75 cm and corresponded to the centre of the test aquarium. Different scenarios (trials) consisting of coral pinnacles (healthy or bleached) as well as animated fish of various species were added to the baseline 3D environment, depending on the simulation, on the left or right side of the aquarium, at a distance of 50 cm. Simulated shoals of five fish could either swim in place on either side or follow a tangent trajectory at a given speed. We used Epic Games Unreal Engine 4.23 (https://www.unrealengine.com/) to render the virtual fish and scene according to the desired test conditions, and to manage the sequencing of trial executions. Fig. 2a shows how three live postlarvae view a virtual scene of corals and adult surgeonfish from within their focal aquarium.

Video-based Tracking

A Microsoft Kinect Azure depth camera was placed 50 cm above the water surface to continuously monitor postlarval fish behaviour in the focal aquarium (Fig. 1b). For each trial, a top-view colour video was recorded and processed in real time at a frequency of 5 Hz to compute the 2D location of each postlarval fish. In the original design of the set-up, we planned to track real-time 3D positions of fish with the infrared (IR) sensor of the Microsoft Azure Kinect depth camera. However, we found that this technology was not suitable for underwater tracking due to the large hot spot created on the surface of the water by the IR grid spot. For this reason, we switched to the colour sensor and could not adjust in real time the rendering viewpoint according to fish position in the aquarium. The detection pipeline, illustrated in Fig. 1c, used both the OpenCV image-processing library (https://opencv.org/) and the Kinect Azure SDK (https://docs.microsoft.com/en-us/azure/Kinect-dk/sensor-sdk-download). Images were extracted from the colour video stream and cropped. The constant background was then removed by subtracting a reference image captured before placing fish in the aquarium. The 2D location of each fish was detected using the OpenCV blob detector with parameters adjusted appropriately. The computer performing the virtual rendering also executed this processing pipeline in real time. The processing had no impact on the frame rate of the visual scene. Tracking performance is provided in Appendix Fig. A1.

Tracking Postprocessing

The 2D positions of blobs, representing individual postlarvae in the group of five, were detected at a sampling rate of 5 Hz. This automated process is not error free: in some frames, fewer than five blobs were detected (low signal for smaller juveniles swimming at greater depth or due to overlaps) or more than five blobs (fish reflecting on the Plexiglas when swimming close to the aquarium sides). The tracking postprocessing pipeline using Python scripts involved seven steps (Fig. 1d). First, frames for which only one or two fish were detected were removed to reduce group mean value noise. Second, reflection biases mentioned above were limited by removing the outermost blob when a pair of fish and wall-reflected fish was potentially detected (i.e. when two vertically or horizontally aligned blobs were very close to each other and to the edge of the aquarium). Third, as the automated detection cannot identify and track individual fish from one frame to the next (identification problem), a minimal heuristic distance was used to track the fish. This distance was only used when the position change of a blob from one frame to the next was minimal (with five individuals, there were 120 possible combinations across each pair of frames). This provided the (partial) trajectories and instantaneous velocities of each individual. Transiently missing or extra blobs could produce artificial jumps to distant locations; above a given distance threshold between frames (corresponding to 15 cm/s) these jumps were ignored in the computation of individual instantaneous velocities. The trajectory reconstructions are plotted with coloured lines for each tracked fish in a (X, Y) square graph representing the aquarium. Fourth, for each validated frame, the X- and Y-positions of the centre of the group, the dispersion relative to the centre (mean distance to the centre) and average individual velocities were computed. To account for the fact that the stimuli were presented either on the right or the left, the sign of the X coordinates was inverted when they presented on the left. Fifth, to visualize the raw results for each experiment and each tested condition, 2D scatterplots with all valid fish positions from all groups and normalized X- and Y-position distribution histograms (with five-pixel bins) were used (a representative scatterplot from experiment 1 is shown in Appendix Fig. A3). Sixth, to visualize the average behavioural responses across time for each experiment and tested condition, heatmaps of fish position density in the aquarium were plotted in successive 1 s intervals. Lastly, the time series for each of the four behavioural measures (group centre X- and Y-position, dispersion and individual velocities) were binned into 5 s intervals

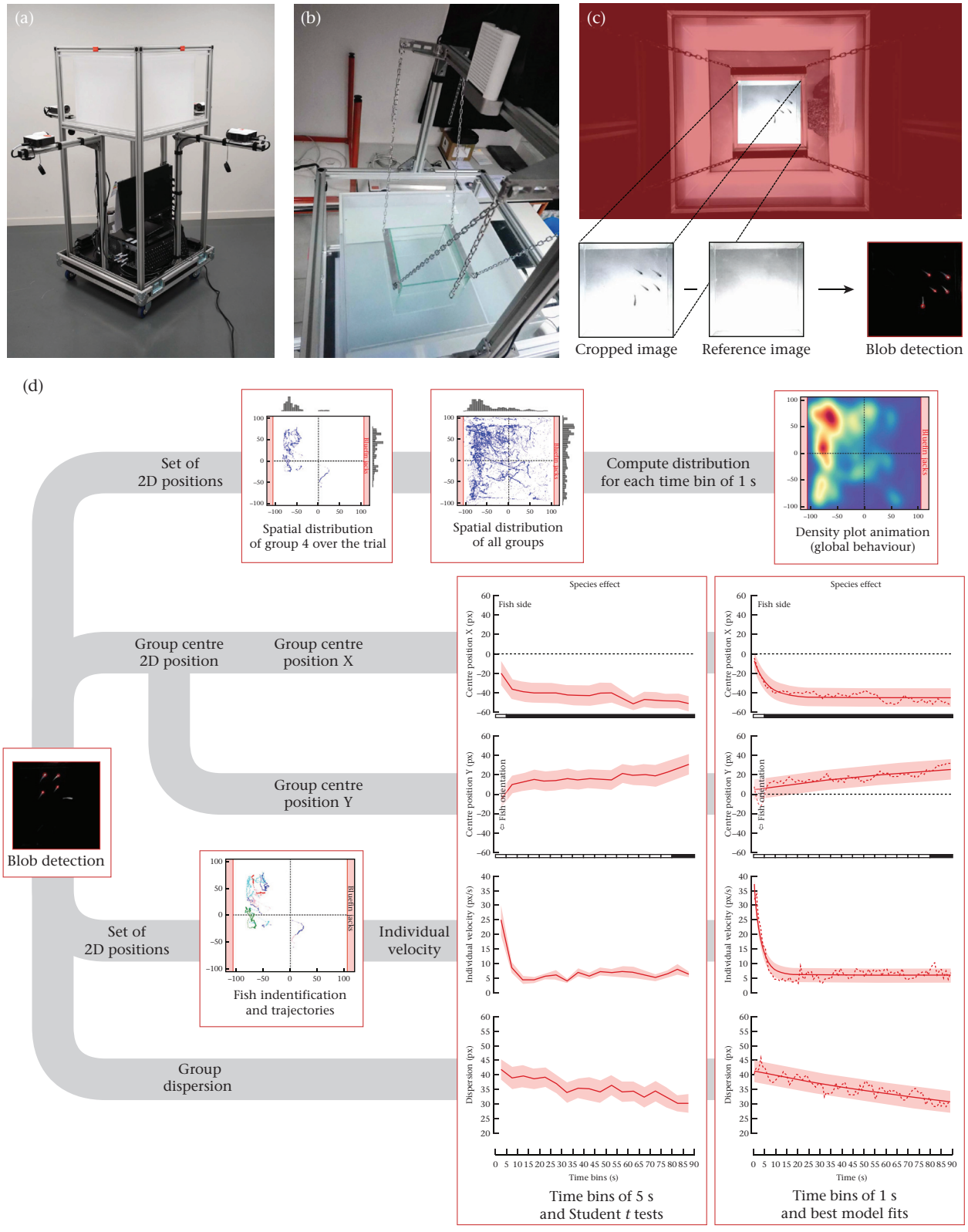

Figure 1. (a) View of the experimental set-up as delivered by Immersion with the test aquarium (dimensions 50 × 50 cm and 35 cm high) and five video projectors (four lateral sides plus bottom). (b) View of the smaller focal aquarium (20 × 20 cm and 20 cm high) placed inside the test aquarium to limit the displacement range of fish, and of the Microsoft Kinect Azure camera recording the behavioural responses. (c) Illustration of the detection pipeline starting from the camera view to blob detection with individual postlarvae executed after cropping and subtracting the reference image, followed by the tracking postprocessing pipeline. (d) Detected 2D positions were used to characterize postlarvae behavioural responses. For each condition, the overall behaviour obtained combining data from all tested groups is visible in the animation of the 2D density heatmaps generated every second. The X- and Y-positions of the centre of the groups, individual velocities and dispersions were averaged across time bins of 5 s to perform statistical comparisons (Student *t* tests), and across time bins of 1 s to fit the behavioural models (regressions). Individual velocities were extracted from the reconstruction of the trajectories, which was based on the identification of each fish from one frame to another (see text).

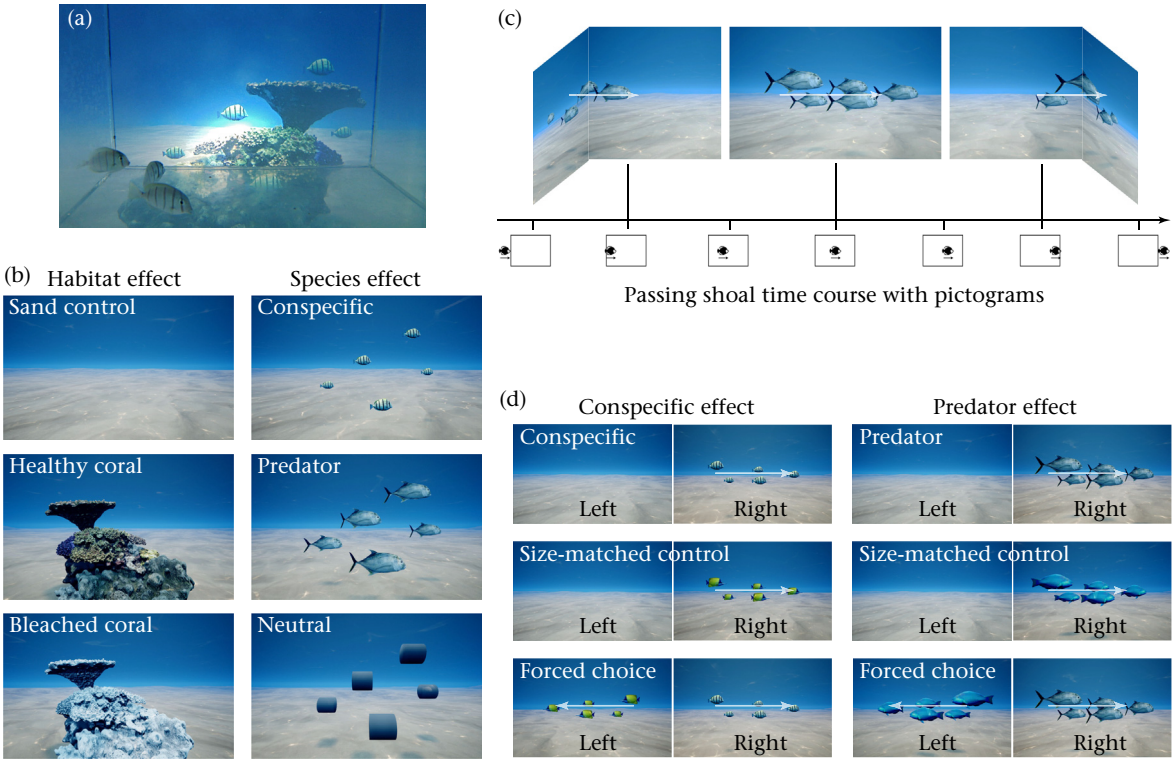

Figure 2. Illustration of the stimuli used in the experiments. (a) Rendered scene with virtual corals and adult surgeonfish as seen from inside the focal aquarium by real larvae. (b) Experiment 1: Habitat effect: Sand control, Healthy or Bleached coral (pinnacles); Species effect: Conspecific (adult surgeonfish), Predator (bluefin jacks), Neutral (untextured cylinders). The fish stimuli were presented in shoals of five individuals swimming in place, centred at a virtual location corresponding to 25 cm behind one of the sides of the test aquarium. (c) Dynamic presentation of a virtual fish shoal swimming past the postlarval fish (either one pass or three passes for experiment 2 and only one pass for experiment 3). The virtual fish species were either conspecifics or predators (as shown here). Shoals swam along a 4.5 m straight line for 30 s at 15 cm/s (slow pace). (d) Experiment 3. Three conditions were tested to examine the response of the postlarval fish to conspecifics: Conspecific alone, Conspecific-sized control alone (butterflyfish) and Forced choice of conspecific versus conspecific-sized control. Three conditions were also tested to examine the response of the postlarval fish to predators: Predator alone, predator-sized Control alone (parrotfish) and Forced choice of predator versus predator-sized control. Similar to experiment 2, the virtual shoals swam along a 6 m straight line for 40 s at 15 cm/s (slow pace).

for the statistical tests, and into 1 s intervals to find the best behavioural model fit.

EXPERIMENTAL VALIDATION

Three main experiments were carried out to understand how postlarval surgeonfish visually recognize a suitable habitat, adult conspecifics and one of their predators (bluefin jacks). Our first objective was to experimentally validate the use of simulated 3D models of fishes in a VR set-up by confirming that they are realistic enough to cause natural reactions in postlarval fish.

Methods

Specimen collection

Over 200 postlarval surgeonfish (total length = 2.55–2.75 cm) were captured using hand nets at night, shortly after they had entered the northeastern reef crest of Moorea, French Polynesia (17°29′52.19″S, 149°45′13.55″W). Individual postlarvae had not yet acquired skin stripes which only form after recruitment; therefore, they were still undergoing metamorphosis, and were considered 'postlarvae' (Besson et al., 2020).

Ethical note

Ethical approval for the study was granted from The Animal Ethics Committee, Centre National de la Recherche Scientifique (permit number 006725). This study also complies with the rules defined by the Direction de l'Environnement de la Polynésie Française (DIREN) regarding experiments on coral reef fish in aquaria. After capture, postlarval fish were placed in acclimatization aquaria at CRIOBE for 36 h, in groups of 40 maximum, filled with UV-sterilized and filtered (10 µm filter) sea water maintained at 28.5 °C, under a 12:12 h light:dark cycle. Stress was minimized during transport using occluded small aquaria. Once the experiment was over, animals were returned to their natural habitat.

Experimental protocol

The behavioural response to the multiple trials, that is, different habitats or fish shoals, was assessed for groups of five postlarval fish placed together in the aquarium. A neutral, baseline 3D environment (sandy bottom with animated caustics) was displayed throughout the experimental sessions on all five sides of the aquarium. Virtual fish or coral pinnacles appeared and disappeared at specific times and in specific virtual locations depending on the trial. Each experiment started with a 4 min habituation period in the baseline environment, followed by trials each lasting 90 s (experiment 1 and 2) or 60 s (experiment 3). To minimize interference, the baseline environment was also displayed for 2 min between trials. For each experiment, the presentation order of trials was randomized and balanced to avoid order effects and allow for statistical comparisons between pairs of conditions. To exclude possible side biases from the random sand texture pattern or from the room's ceiling and lighting, the stimulus side was randomly balanced between the left and right of the aquarium. Lastly, after

every half-day the aquarium was emptied, washed with freshwater and refilled, and the focal aquarium was oxygenated between replicates.

Experiment 1: Effects of static presentation of habitat and fish. Groups of five postlarval fish were presented with six trials: three virtual habitats and three virtual fish or neutral shapes on only one side of the aquarium (randomized) each for 90 s (Fig. 2b). Virtual simulations rendered the postlarval fish at a depth of 1.25 m. The three virtual habitats tested were Sand control (only the sandy baseline environment), Healthy coral (a pinnacle with healthy tabular and branched corals) and Bleached coral (the same pinnacle, but all corals were bleached). The three virtual fish species consisted of shoals of five virtual fish swimming in place in the same pattern and position: Conspecifics (five adult surgeonfish), Predators (five bluefin jacks) and Neutral (five large untextured cylinders). The individual positions of five postlarval fish were constantly tracked during the six successive trials presented in the following order: Sand control (first); Healthy or Bleached coral (randomly second or third); Conspecific, Predator or Neutral (randomly fourth, fifth or sixth). Sixty postlarval fish were tested in 12 groups of five fish, and for each the total experimental duration was approximately 22 min.

Experiment 2. Effects of static versus dynamic presentation of fish. In experiment 2, with eight trials, behavioural responses to the static presentation of shoals of five virtual fish were compared with behavioural responses to a more realistic dynamic situation in which shoals of five fish appeared, swam past the postlarval fish in a nonaggressive manner and disappeared. Three virtual fish shoal trials were projected: one static shoal swimming in place (as in experiment 1) for 90 s; one shoal swimming by during the first 30 s, then disappearing, followed by 60 s of the baseline sand environment; or three successive shoals of five fish swimming nearby and disappearing, each over 30 s. In each, virtual shoals swam for 30 s at 15 cm/s (slow pace) along a virtual line placed 115 cm from the centre of the test aquarium, covering a total distance of 4.5 m (Fig. 2c). The virtual fish shoals were either surgeonfish conspecifics or bluefin jack predators and were presented in eight successive trials in the following order: Sand control (first); Conspecific/Predator static, one pass or three passes (randomly presented in second, third or fourth position); Sand control (fifth); Conspecific/Predator static, one pass or three passes (randomly presented in sixth, seventh or eighth position). The order in which the fish shoal was presented (conspecifics or predators first) was varied and the side of the aquarium on which the virtual fish were presented was randomized. Sixty postlarval fish were tested in 12 groups of five postlarvae, and for each the total experimental duration was approximately 26 min.

Experiment 3. Effect of size-controlled dynamic presentation of fish. In experiment 3, behavioural responses to a dynamically swimming shoal of conspecifics or predators was compared with behavioural responses to size-matched heterospecifics. Six virtual fish shoal trials were projected (Fig. 2d): surgeonfish conspecifics on one side; conspecific-sized control fish on one side (butterflyfish, *Forcipiger longirostris*); conspecifics and conspecific-sized controls on opposite sides (two-alternative choice); bluefin jack predators on one side; predator-sized control fish on one side (parrotfish, *Scarus psittacus*); predators and predator-sized controls on opposite sides (two-alternative choice). Changes in postlarval fish positions from before to after a virtual shoal swam by were identified. All virtual fish swam at 15 cm/s (slow pace) for 40 s along a virtual line placed at 115 cm from the centre of the aquarium (total distance travelled: 6 m). The order in which fish shoal types were presented, conspecifics or predators, was balanced between groups; however, the two-alternative choice was always presented after the single-choice trials. The order of single-choice trials was also balanced. In all conditions, the stimulus was presented over 40 s, and postlarval position recording started 10 s before and ended 10 s after the stimulus (total duration of 60 s). Eighty postlarval fish were tested in 16 groups of five fish, and for each the total experimental duration was approximately 26 min.

Data analysis

For all experiments, tracking data were sampled at 5 Hz, during 90 s trials for experiments 1 and 2 and 60 s trials for experiment 3 (see Fig. 1c). Representative trajectories of postlarval groups are available in Appendix Figs A2, A5 and A7 for experiments 1, 2 and 3, respectively. Animated heatmaps of fish position density in the aquarium for all conditions are available in Supplementary Videos A1, A2 and A3 for experiments 1, 2 and 3, respectively. Note that for all 2D plots, data are organized so that the stimulus is always presented on the right side, except for the forced-choice conditions of experiment 3, for which stimuli are presented on both left and right sides. General repeated-measures ANOVAs with trial and 5 s time bin as main factors were generated using the four behavioural measures (group centre X- and Y-position, dispersion and individual velocity). Comparisons between relevant trials (paired Student *t* tests) and the deviation from zero of the group's X- and Y-positions (Student *t* tests against a single value of 0) were conducted for each time bin. The alpha value for significance was adjusted using Bonferroni's correction for multiple comparisons on a single data set (see figure legends for visualization). Plots displaying the time series of the four behavioural measures (binned in 5 s intervals) and the results from the statistical comparisons are provided in Appendix Figs A4, A6 and A8 for experiments 1, 2 and 3, respectively.

Behavioural model fit

To characterize the temporal aspect of postlarval fish behavioural responses, we designed several models taking the distance of the postlarval fish to the simulated shoals into account. The position of the virtual simulations was sustained and constant throughout the trials in experiment 1 and in the static trials of experiment 2, but the virtual shoals moved in the dynamic conditions of experiments 2 and 3. Because of this major difference between the static and dynamic conditions, we used a different set of possible behavioural models for each type of trial to measure behaviour (centre position, individual velocity and dispersion). For the static conditions, we tested three simple ecologically relevant models (linear, quadratic and exponential) and for dynamic conditions, we added a periodic component to capture the cyclic variations of the stimulus (Table 1). The average behavioural measures obtained for the tested groups ($N = 12$ or $N = 16$), binned in 1 s intervals, were fitted using each of the three models. The fit quality was estimated with the root mean square error (RMSE) between the average data points and the model predictions. To avoid data overfitting, we used a limited number of models and selected the best model based on the trade-off between fit quality (RMSE) and the number of parameters. Linear models (for static conditions) and linear periodic models (for dynamic conditions) have one parameter fewer than the quadratic and exponential models. They were favoured when the RMSE difference with the other models was below 5% (e.g. if the linear and quadratic fits had RMSEs of 10 and 9.6 respectively, the linear model was selected). Lastly, to check the validity of each fit, the obtained RMSE was compared to the RMSE distribution obtained by applying, for the given condition and measure, the same fitting procedure but with scrambled time bins 1000 times. Two quality criteria were used: if the obtained RMSE

Table 1
The sets of behavioural models fitted for the static and dynamic trials

Name	Equation	Description and meaning of the parameters
Static conditions		
Linear	$at+b$	Linear models capture responses that change constantly in time. These drifts can be observed in slow responses to a potential danger. a: linear term (drift speed) b offset (start position)
Quadratic	at^2+bt+c	Quadratic models capture responses that change constantly in time (first order) and that have a reversal (second order). Reversals are observed after a loss of interest when attracted by the stimulus ($a<0$ if on right side) or after habituation to a fearful stimulus ($a>0$). a: quadratic term (reversal) b: linear term (drift speed) c: offset (start position)
Exponential	$l-(l-s)\exp(-kt)$	Exponential attenuation models capture natural decaying phenomena within a limited spatial or temporal range. These can be observed in quick escape response to a fearful stimulus. l: limit of the attenuation (reached when $t\rightarrow\infty$) s: offset (starting position) k: attenuation factor (positive value, higher for faster decays)
Dynamic conditions		
Linear periodic	$at+b+\frac{1}{2}A\cos(2\pi(t-t_0)/T)$	Linear models combined with a periodic component capture linear drift responses to a cyclic stimulus. Periodic component parameters: A: amplitude of the oscillations (positive value) t_0: phase of the oscillations (peak time, within [0 s, T]) T: period (fixed parameter set to 30 s and 40 s for experiments 2 and 3)
Quadratic periodic	$at^2+bt+c+\frac{1}{2}A\cos(2\pi(t-t_0)/T)$	Quadratic models combined with a periodic component capture first- and second-order responses to a cyclic simulation
Exponential periodic	$l-(l-s)\exp(-kt)+\frac{1}{2}A\cos(2\pi(t-t_0)/T)$	Exponential attenuation models combined with a periodic component capture naturally decaying periodic responses to a cyclic simulation

For each model, the equation, the description of the behaviour that it captures and the meaning of its parameters are detailed.

was lower than 0.8 times the mean RMSE distribution, and below the lower 1% confidence interval bound of the distribution, the fit was considered valid (good signal-to-ratio level). The results are summarized in plots displaying, for each condition, the time series of each measure in bins of 1 s, the best behavioural model fit and the outcome of the statistical comparisons. For each condition, the selected model and adjusted parameters are detailed in Appendix Tables A1, A2 and A3 for experiments 1, 2 and 3, respectively.

Results

Experiment 1. Effects of static presentation of habitat and fish

The behavioural responses to the trials were assessed for groups of five postlarval surgeonfish placed together in the aquarium. All trials were tested on all groups of postlarval fish. Typical individual trajectories of postlarval fish in response to each of the six trials are shown in Appendix Fig. A2, scatterplots with all positions occupied by all postlarval fish in Appendix Fig. A3, and animated heatmaps with the presence density at each successive 1 s intervals in Supplementary Video A1.

Habitat effect. Postlarval fish reactions were similar across habitat types (Sand control, Healthy and Bleached coral). Postlarval fish group centre's X- and Y-positions were not significantly different between trials either over the whole test period or for most 5 s intervals (lack of significance in boxes below plots in Fig. 3a, b). Apart from a small positive bias (16.5 px) in the Y-position for the Sand control (entire range: $t_{11}=2.39$, $P<0.04$), possibly related to the initial location in which fish were placed in the aquarium, the X- and Y-positions were not biased to either side of the aquarium (Fig. 3a, b). The level of noise did not allow for good quality fits of linear, quadratic or exponential models (Table A1), but the best fit models largely overlapped, confirming nonsignificant differences in response behaviours across habitat types. In contrast, there was a significant effect of habitat on individual velocities ($F_{2,22}=5.5$, $P<0.015$, $\eta^2_G=0.12$), with postlarval fish moving faster (more activity) when presented with Healthy (23.8 px/s, $t_{11}=2.26$, $P<0.05$) and Bleached (23.7 px/s, $t_{11}=3.11$, $P<0.01$) corals compared to no corals in the Sand control (14.7 px/s) over the whole time range and during some of the 5 s intervals (shaded boxes below plot in Fig. 3c). No significant difference in group dispersion, with either statistics or model fitting, was observed across habitat types (Fig. 3d).

Species effect. Postlarval fish reactions did not differ when presented with static shoals of conspecifics (surgeonfish) and neutral cylinders but were significantly different when presented with predators (jack fish). Type of fish shoal impacted the postlarval fish group centre's X-position (main effect, $F_{2,22}=8.3$, $P<0.002$, $\eta^2_G=0.27$), which was significantly lower with Predators (−42.3 px) than with Conspecifics (−1.5 px, $t_{11}=3.14$, $P<0.01$) or Neutral cylinders (1.8 px, $t_{11}=3.7$, $P<0.005$) across the entire time range and for most 5 s intervals (shaded boxes below plot in Fig. 3e). Postlarval fish swam away from the virtual predators: they moved 31.6 px from the first to the last time bin ($t_{11}=2.83$, $P<0.02$), mostly at the beginning of the trial (exponential model with k parameter of 0.17/s). On the other hand, with virtual conspecifics postlarval fish hit the sides of the aquarium near the conspecifics more often than with Neutral cylinders or Sand. There was no global effect of the type of virtual species on postlarval fish Y-positions across the entire time range and for any interval (Fig. 3f). However, postlarval fish moved slowly towards the upper-left quadrant of the aquarium, the opposite side to the simulation, and moved to the back of the virtual shoal (linear model with a slope of $a=0.238$ px/s) moving 36.5 px ($t_{11}=3.09$, $P<0.01$) behind the virtual predators, reducing dispersion (Supplementary Video A1). Type of fish shoal had a significant effect on individual velocities ($F_{2,22}=11.08$, $P<0.001$, $\eta^2_G=0.20$), with lower speeds with Predators (7.3 px/s) than with Conspecifics (20.9 px/s, $t_{11}=4.09$, $P<0.002$) and Neutral cylinders (19.3 px/s, $t_{11}=3.23$, $P<0.01$) over the entire time range and most 5 s intervals (Fig. 3g).

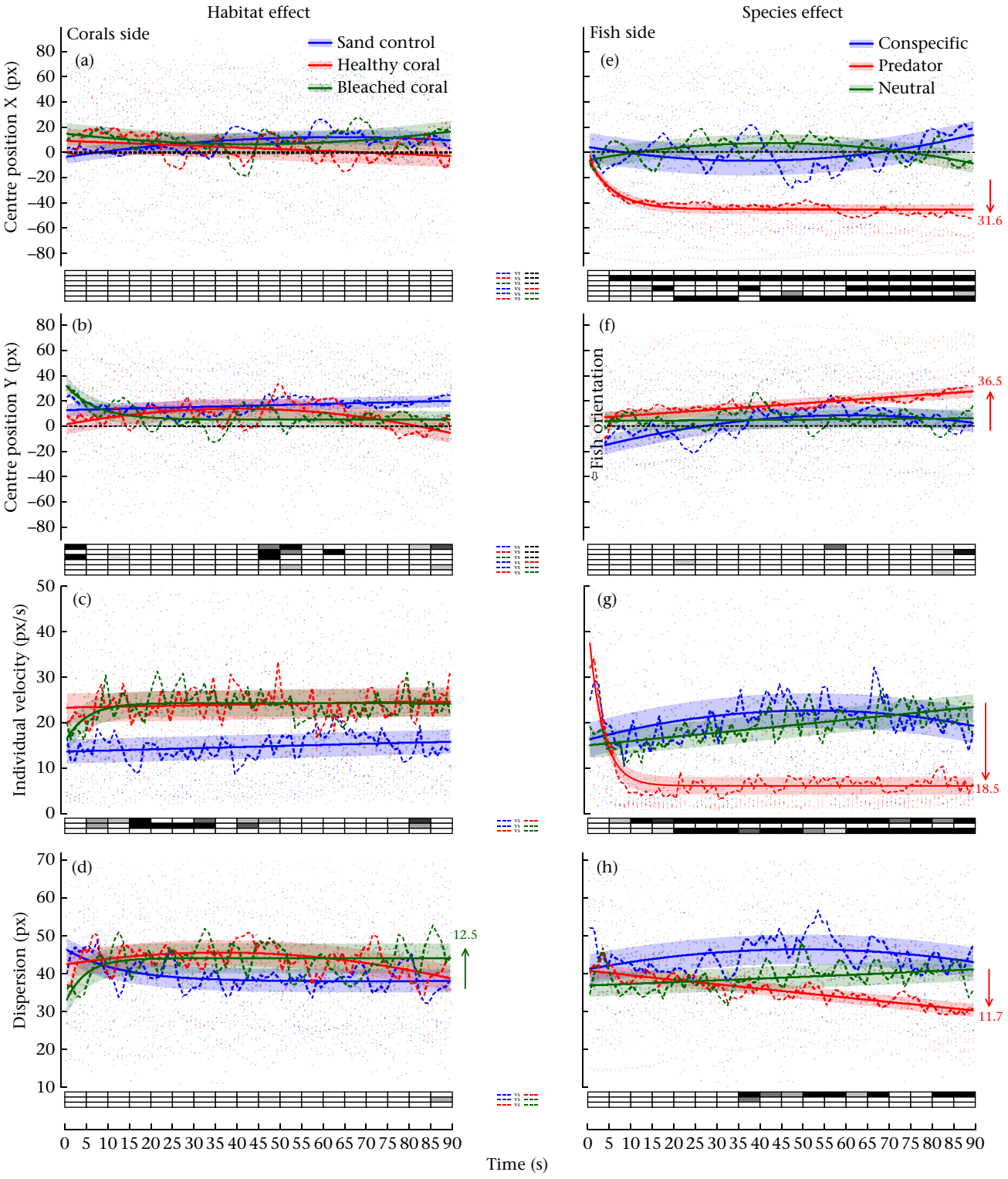

Figure 3. Experiment 1 group time series, with best model fits and statistics. X- and Y-positions of the group centre, individual velocity and group dispersion are shown for (a–d) habitat and (e–h) species trials. Coloured dashed lines show the average at each time point of $N = 12$ groups (Habitat trials: Sand control in blue, Healthy coral in red, Bleached coral in green; Species trials: Conspecific in blue, Predator in red, Neutral in green). Coloured lines show the best fitting model for the corresponding trials and error stripes show the RMSE. For each 5 s time bin, average performances were compared either between each trial or to zero with paired and single-value Student *t* tests. Significance levels are provided in the boxes below the plots (ranging from light grey for $P < 0.05/1$ to black for $P < 0.05/N_{Tests}$ using Bonferroni's correction for $N_{Tests} = 3$; white for $P > 0.05$).

Furthermore, with Predators individual velocities rapidly decreased by 18.5 px/s over the first 10 s ($t_{11} = 3.47$, $P < 0.005$), remaining at 6.1 px/s until the end of the trial (exponential model with a very high *k* parameter value of 0.30/s). Movement, as well as space occupied in the aquarium, were similar with Conspecifics, Neutral cylinders or Sand (Appendix Fig. A3). The effect of fish shoal type on group dispersion was nearly significant ($F_{2,22} = 2.89$, $P = 0.077$, $\eta^2_G = 0.071$), due to less dispersion with Predators (35.5 px) than

with Conspecifics (44.9 px) across the entire time range ($t_{11} = 3.37$, $P < 0.007$), and in most intervals after 35 s (Fig. 3h). With Predators, group dispersion decreased slowly and progressively during the trial (linear model with $a = -0.12$ px/s), by 11.7 px ($t_{11} = 2.90$, $P < 0.015$): postlarval fish tended to gather after detecting a threat. The best fitting models of the behavioural reactions to Predators highlight natural repulsion from a fear-eliciting stimulus: the exponential models captured quick responses in a limited space/time range (X-position and individual velocity), whereas the linear models captured slow drifting responses (Y-position and dispersion). In general, the four different behavioural indicators (X- and Y-position, individual velocity and dispersion) did not differ between Conspecifics and Neutral cylinders, and despite high variability between individuals resulting in poor quality fits, models also mostly overlapped (Appendix Table A1). However, with Predators, the quality of model fitting for all behavioural measures was excellent i.e. postlarvae showed homogeneous behaviours within each group as well as across groups.

Experiment 2: Effects of static versus dynamic presentation of fish

Typical individual trajectories of postlarval surgeonfish in response to each of the eight trials are shown in Appendix Fig. A5, and animated heatmaps with the presence density at each successive 1 s interval in Supplementary Video A2. Sand control trials were presented before the Conspecific and Predator trials to provide acclimatization periods. Since no qualitative or statistical differences in behaviour were observed, these results are not reported here.

Conspecific effect. Postlarval fish reactions were different when presented with either static (swimming in place) or dynamic (one or three passes) surgeonfish. In the static trial, groups came close to the simulation (hitting the aquarium side), similarly to experiment 1, and the group centre's X-position did not deviate significantly from zero. The best fitting, quadratic, model was only of average fit but its positive a parameter suggested habituation to an initially slightly fear-eliciting stimulus (Fig. 4a, Appendix Table A2). In contrast, in the dynamic one-pass or three-passes trials, postlarval fish joined and moved with the virtual surgeonfish shoal as it travelled along the aquarium side (oscillating X- and Y-positions, Fig. 4a, b). When the shoal passed three times, postlarval fish kept repeating the same behaviour periodically, without any noticeable attenuation, indicating no loss of interest (Supplementary Video A2). The linear periodic model was the best fit, as it captured the postlarval fish cyclic response, with a phase t_0 of approximately 17 s for both one-pass and three-passes tests, and an amplitude A of 21.6 px (one pass) and 24.7 px (three passes). The linear component had an offset b of about 14 px for both pass types and a slope a of −0.13 px/s (one pass) and null (three passes). Oscillations in the X-position showed a significant deviation from zero towards the simulation side when the shoal was passing (from 15 to 25 s for both one and three passes, and from 45 to 55 and 75 to 85 s for three passes). For the static trial the group centre's Y-position did not deviate significantly from zero and the best fit was exponential, but of poor quality (Fig. 4b). For the one-pass trial, the linear periodic model had the best fit, with a similar phase ($t_0 = 15.6$ s) but with a much smaller amplitude ($A = 8.5$ px) than for the X-position. The number of postlarval fish that followed the single shoal passage (Supplementary Video A2) was too limited to produce a clear trough, resulting in less vertical motion. Moreover, the linear decay and loss of synchronization in the model after the first cycle was due to the absence of stimuli after 30 s. For the three-passes trial, the best fitting model was exponential and periodic, with a strong attenuation factor of $k = 0.177$/s, rapid oscillations around $l = 7.7$ px, a peak at $t_0 = 13.2$ s and large amplitudes ($A = 41.8$ px; Fig. 4b). The first two oscillations showed significant deviations from zero on peaks and troughs. The X- and Y-oscillations were synchronized and phase-locked with the three virtual surgeonfish shoal passes: vertical motion overlapped widely with the shoal's linear displacement along the aquarium side, and the horizontal motion corresponded to the movement of postlarvae closer to the shoal at each pass. The kinematic analyses of swimming provide evidence of cohesive group behaviour, in which larvae naturally recognize and follow their conspecifics. Individual velocities were rapidly and significantly lower (at 12 px/s then increased linearly, with a fitted slope of 0.064 px/s) with static compared to dynamic virtual conspecifics (Fig. 4c). This is consistent with an initially slightly fearful response. In dynamic trials, individual velocities oscillated around 20 px/s and decreased to similar values as in static trials towards the end of the trial, but noise was too high for the periodic models to reach a good fit (Appendix Table A2). Group dispersion tended to be lower for the static than dynamic trials, and fit was poor (Fig. 4d).

Predator effect. Postlarval fish reacted very differently to static compared to dynamic bluefin jack shoals. Static presentation produced the same reaction as in experiment 1: movement to the opposite side and to the back of the virtual shoal with reduced group dispersion. In the one-pass or three-passes dynamic tests, the density patterns of heatmaps were bimodal, indicative of two reaction types: one similar to that of the static trial, while the second was an asynchronized back-and-forth movement in the X-dimension with the postlarvae moving behind the virtual predators after each pass. The balance between these two reactions varied, with the proportion of static-like behaviour increasing through time. In the static condition, the gradual decrease in X-position (significant deviation from zero in all time bins beyond 30 s) was best fitted with a quadratic model ($a = 0.006$ px/s^2, $b = -0.96$ px/s and $c = -4.3$ px), with parameters for the climax and reversal outside the trial time range (Fig. 4e, Appendix Table A2). The best fitting model for the three-passes condition was linear periodic, with peaks occurring earlier than with conspecifics ($t_0 = 12.8$ s), a limited amplitude ($A = 14.6$ px) and a linear drift (slope $a = -0.404$) of postlarval fish that gradually moved to the opposite aquarium side. For the one-pass trial, the response to the first pass overlapped with that of the three-passes ($t_0 = 12.7$ s and $A = 9.5$ px) and after this pass, oscillations and drifting were exponentially attenuated. None of the X-positions in the dynamic scenario deviated significantly from zero, but postlarval fish were significantly closer to the stimulus side than in the static trial over multiple time bins. The Y-position was very similar in the three trials (Fig. 4f): postlarvae moved rapidly behind bluefin jack shoals whether swimming in place (quadratic model) or passing nearby once (quadratic periodic) or three times (exponential periodic). Despite good quality fits, these models largely overlapped and deviated significantly from the midline zero in almost every time bin after the first 5 s. At the end of the trials, postlarvae tended to move back towards the midline in the static condition (habituation) and in the one-pass condition (no more simulation). Consistent with experiment 1, individual velocity in the static trial decreased rapidly from 21.3 px/s ($k = 0.50$/s) to 8.2 px/s, which matched an exponential attenuation model (Fig. 4g). In the three-passes condition, postlarval velocities fitted an exponential periodic model, decreasing rapidly from 19.4 px/s ($k = 0.27$/s) to oscillate around 12.4 px/s at small amplitude ($A = 2.6$ px). Furthermore, velocities decreased when postlarval fish noticed predators at each new pass (peak phases locked to $t_0 = 6.5$ s). In the one-pass trial, oscillations had a lower amplitude ($A = 1.5$ px), and individual velocities increased linearly after the shoal pass, with underlying oscillations starting once speeds exceeded 10.9 px/s. The only difference

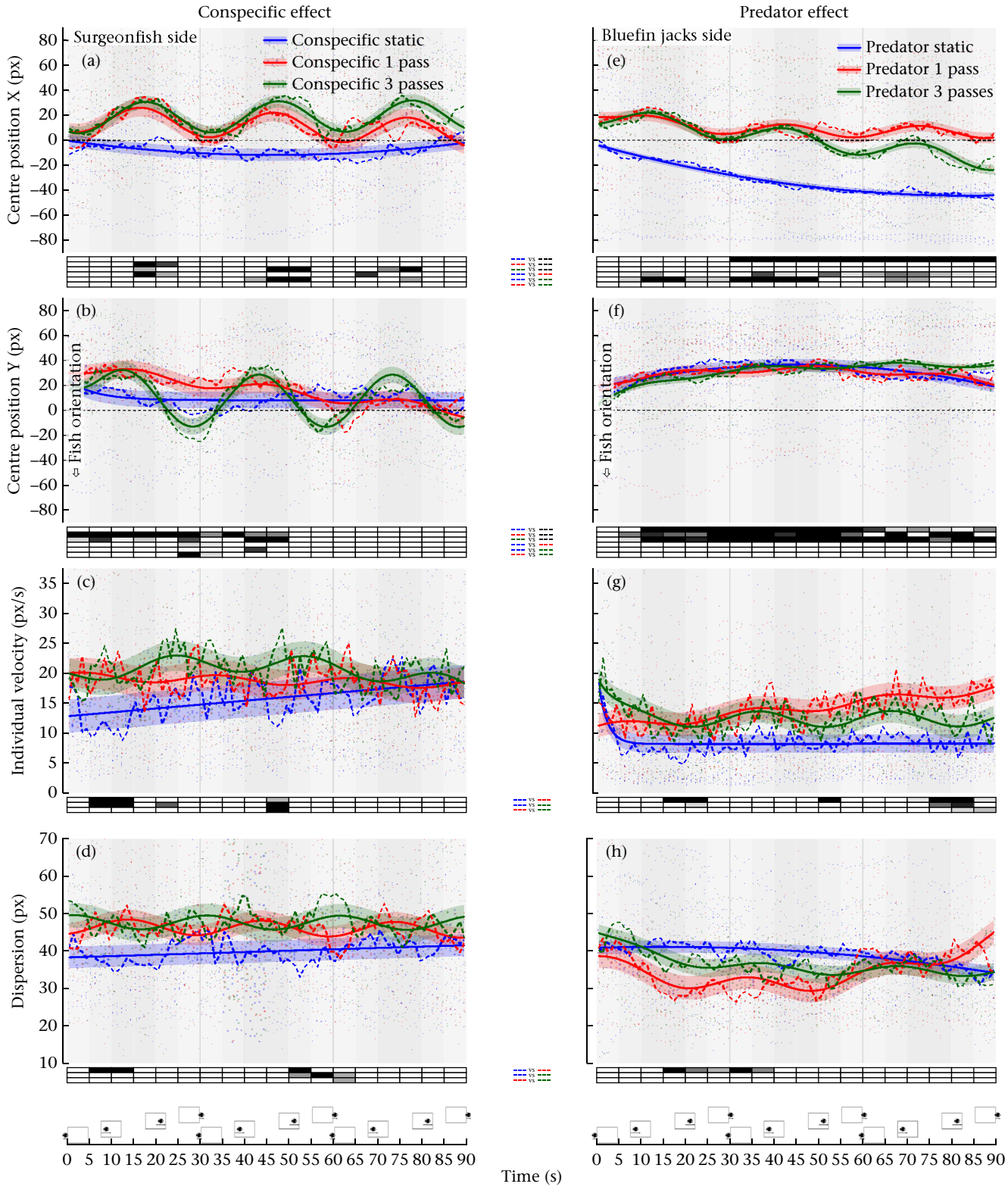

Figure 4. Experiment 2 group time series, with best model fits and statistics. X- and Y-positions of the group centre, individual velocity and group dispersion are shown for (a–d) Conspecific and (e–h) Predator trials. Coloured dashed lines show the average at each time point of $N = 12$ groups (Conspecific and Predator trials: static in blue, one pass in red, three passes in green). Coloured lines show the best fitting model for the corresponding trials and error stripes show the RMSE. For each 5 s time bin, average performances were compared either between each trial or to zero with paired and single-value Student t tests. Significance level is provided in the boxes below the plots (ranging from light grey for $P < 0.05/1$ to black for $P < 0.05/N_{Tests}$ using Bonferroni's correction for $N_{Tests} = 3$; white for $P > 0.05$). Shaded areas highlight the stimuli-critical periods based on the ongoing distance of the virtual shoals in the three-passes conditions (30 s periodicity) illustrated by the fish positions relative to the side screen shown above the time axis.

between trials occurred towards the end of the static and one-pass trials, when postlarval fish swam faster in the absence of the stimulus. Group dispersion was lower for the dynamic one-pass than for static trials (15–40 s; Fig. 4h), increasing again in the absence of the stimulus (quadratic periodic model). In the static trial, dispersion decreased slowly (quadratic model) but less than in experiment 1, possibly due to the influence of dynamic trials used in the design. In the three-passes trial, dispersion was exponentially attenuated, starting at 45 px dropping almost linearly to 34 px (low k factor of 0.06/s).

Experiment 3. Effect of size-controlled dynamic presentation of fish

Typical individual trajectories of postlarval surgeonfish in response to each of the six trials are shown in Appendix Fig. A7, and animated heatmaps with the presence density at each successive 1 s interval in Supplementary Video A3. In contrast to previous experiments, model fitting was limited to the interval of 10–50 s, during which the stimulus was visible: the cycle duration of the periodic component was set to 40 s.

Conspecific effect. Postlarval fish reactions to virtual conspecific surgeonfish or control size-matched butterflyfish passing nearby were mostly similar, yet with subtle differences. Postlarval fish showed the same behaviour as in experiment 2: they moved to the upper-right quadrant, but fewer of them followed the virtual shoal of nonaggressive size-matched controls along the Y-axis than they did with conspecifics. Further, dispersion increased faster in the Control than in the Conspecific trials. When both conspecifics and controls were presented (Forced choice), most postlarval fish gathered on the conspecific side and followed the shoal. The best model for all conditions was linear periodic, except when stated otherwise (Appendix Table A3). The linear components of the change in X-positions in the Conspecific and Control trials were positive, suggesting an increase in interest over the trial (Fig. 5a). However, the oscillation during the single pass had a larger amplitude and peaked a few seconds later for surgeonfish ($A = 45.7$ px and $t_0 = 31$ s) than control butterflyfish ($A = 26.3$ px and $t_0 = 24$ s). The time interval during which the X-position deviated significantly from the midline was longer for conspecifics (more than three time bins compared to one) and there was a significant difference in X-position between the Control and Conspecific trials during the 35–40 s interval. The linear component of the Y-position in both the Conspecific and Control trials had the same positive slope ($a \approx 0.4$ px/s) and oscillation phase ($t_0 \approx 26$ s), but the amplitude in the Conspecific trial was smaller ($A = 26$ px against 46 px; Fig. 5b). The Y-position did not deviate from the midline and was significantly higher in the Control trial. When both fish shoals were presented (Forced choice), postlarval fish responses were less intense than when presented with only one stimulus but still showed the same two reaction types, that is, following the conspecifics or remaining in the upper-left quadrant. The X-position was positive and peaked at $t_0 = 38$ s, but deviation from the midline was not significant due to a strong linear decrease ($a = -0.92$). Together, these results indicate that postlarval fish were more attracted to and followed conspecific surgeonfish, while spending more time in the upper-right quadrant with similarly sized butterflyfish. Individual velocity measurements were noisy but remained relatively constant throughout the three trials (at 30 px/s), with fits that mostly overlapped (Fig. 5c). The linear component of the good quality fit group dispersion model was similar in all three trials, with a nearly null slope (constant) at $b \approx 50$ px (Fig. 5d). There were differences in the periodic component, with oscillations of smaller amplitude and troughing 6 s later with Conspecifics ($A = 6.6$) compared to Controls ($A = 12.2$ px), confirming that dispersion increased faster after the butterflyfish shoal passed than after the conspecifics.

Predator effect. Heatmaps of postlarval fish position density highlight subtle differences in their reaction to dynamic virtual predators versus control parrotfish. With predators, postlarval fish rapidly moved to the upper-right quadrant and remained at the back of the shoal. In contrast, with nonaggressive size-matched controls, postlarval fish also gathered in the upper-right quadrant, but some rapidly started to follow the shoal: group dispersion increased more and earlier than with predators. When both predators and nonaggressive controls were presented (Forced choice), most postlarval fish gathered in the upper-left quadrant with controls, with only a few staying on the predator side or following either predators or controls. The periodic component of the X-position for the Predator trials was smaller and peaked earlier ($A = 36.9$ px and $t_0 = 29.7$ s) than for Control trials ($A = 41.6$ px and $t_0 = 32$ s; Appendix Table A3): with bluefin jacks, postlarval fish moved more and earlier to the stimulus side (20–35 s) than with parrotfish (30–35 s; Fig. 5e). When both fish shoals were presented (Forced choice), the X-position of postlarval fish fluctuated around the midline ($b = -19.4$ px and $A = 25.1$ px), with a nonsignificant deviation towards parrotfish. The periodic component of the Y-position peaked for all conditions at similar times ($t_0 = 24.2$–29.6 s), with postlarval fish moving rapidly behind fish shoals (Fig. 5f), especially with predators. However, the combined periodic amplitude and quadratic component in the Predator trials, and the linear component in the Forced choice task, indicated that, while postlarval fish tended to follow parrotfish and were distributed centrally along the Y-axis at the end of the simulation (deviating from the midline only in the 25–35 s interval), they remained in the upper-half of the aquarium behind virtual predators (Y-position always positive throughout the simulation). Across the three trials, individual velocities decreased rapidly to about 20 px/s, with troughs at similar times ($t_0 = 22.8$–25.8 s). However, the model fit of velocity had a quadratic component highlighting that velocity decreased over a longer period of time in the Predator than the Control trials before increasing again (Fig. 5g, Appendix Table A3). Dispersion decreased earlier than velocities and increased slower with Predators (trough at 35.5 s) than Controls (trough at 31.9 s) although this was not statistically significant (Fig. 5h).

Discussion

Virtual corals, healthy or bleached, displayed on one aquarium side had a significant effect on postlarval fish behaviour (Fig. 3a–d). Postlarval fish increased their swimming speed and spent more time close to the aquarium side displaying the simulated corals compared to sand controls with no corals. Interestingly, both healthy and bleached corals attracted postlarval fish. As herbivores, corals are not part of the diet of surgeonfish, so this attraction may be due to anfractuosities in the coral framework, potentially providing shelter and/or a hiding place (Leis & McCormick, 2002). In addition, displays of virtual fish highlighted clear and distinct behavioural responses in postlarval surgeonfish (Fig. 3e–h). When presented with five virtual 3D adult conspecifics, postlarval fish were attracted to them within 10–20 s. In contrast, when presented with their natural predators, five virtual bluefin jacks (Siu et al., 2017), postlarval fish moved to the opposite side of the aquarium with a rapidly decreasing velocity, and then slowly gathered behind the virtual predator shoal. These contrasting responses highlight the ability of these postlarval coral reef fish to visually identify virtual conspecifics and predators and respond differently, with either attraction (conspecifics) or repulsion and/or avoidance (predators), consistent with expectations from natural behaviours.

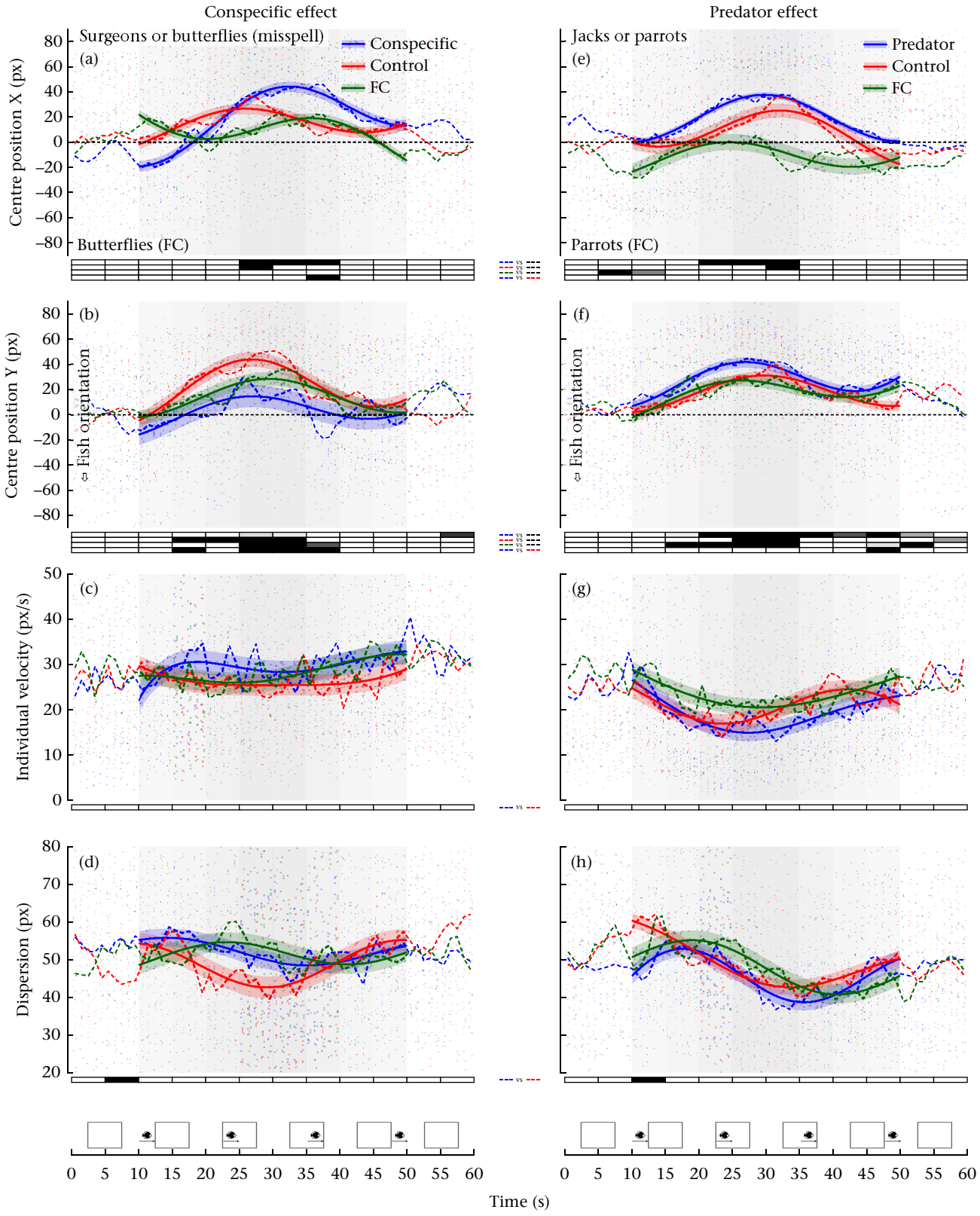

Figure 5. Experiment 3 group time series, with best model fits and statistics. X- and Y-positions of the group centre, individual velocity and group dispersion are shown for (a–d) Conspecific and (e–h) Predator trials. Coloured dashed lines show the average at each time point of $N = 16$ groups (Conspecific trials: Conspecific in blue, Control in red, Forced choice (FC) in green; Predator trials: Predator in blue). Coloured lines show the best fitting model for the corresponding trials and error stripes show the RMSE. For each 5 s time bin, average performances were compared either between each trial or to zero with paired and single-value Student *t* tests. Significance level is provided in the boxes below the plots (ranging from light grey for $P < 0.05/1$ to black for $P < 0.05/N_{Tests}$ using Bonferroni's correction for $N_{Tests} = 3$; white for $P > 0.05$). Shaded areas highlight the stimuli-critical period based on the ongoing distance of the passing virtual shoals illustrated by the fish positions relative to the side screen shown above the time axis.

Furthermore, the movement of postlarval fish behind the predator shoal not only confirms their recognition of the virtual predator but also of virtual body features (distinguishing head from tail and positioning themselves accordingly).

The presentation of static or dynamically moving conspecifics led to contrasted reactions in postlarval fish (Fig. 4a–d). The sudden appearance of a static conspecific shoal startled postlarval fish, causing them to move away or remain stationary, but then they showed attraction, even hitting the side of the aquarium where conspecifics were displayed. However, when the virtual conspecific shoals appeared 2.5 m away and slowly got closer, no startle responses were observed; rather, postlarval fish followed the virtual shoals along the side of the aquarium, even after three identical passes. This dynamic scenario is particularly interesting as it highlights the postlarval fish's natural cohesive group behaviour, even with virtual conspecifics. Such shoaling and cohesive behaviours with virtual conspecifics have previously been observed in other experiments (e.g. in adult zebrafish, Saverino & Gerlai, 2008). In contrast, when static predators suddenly appeared on one aquarium side, postlarval fish slowly moved to the opposite side of the aquarium and gathered behind the virtual predator shoal (Fig. 4e–h). When virtual bluefin jacks swam by, the reaction of the postlarval fish was less clear across individuals, but mostly consisted of an overall decrease in swimming speed and/or synchronized movements to hide behind the moving virtual predators. When virtual bluefin jacks passed three times, the static-like behaviour became more frequent and individual swimming speeds decreased with each new pass.

We then tested whether these postlarval fish responses were simply due to the size of virtual fish, that is, repulsion from larger fish and attraction to smaller fish, or whether postlarval fish are able to differentiate between virtual fish species. We found subtle yet noticeable differences in postlarval fish reactions to virtual shoals of same-sized nonaggressive controls, butterflyfish and parrotfish, compared to conspecifics (surgeonfish) and predators (bluefin jacks), respectively. Postlarval fish showed stronger and longer-lasting attraction towards conspecifics, with clear shoal-following behaviour and less dispersion, than towards butterflyfish and a preference for conspecifics when both were presented simultaneously (Forced choice; Fig. 5a–d). When presented with predators, the postlarval fish's back-and-forth escape reaction was triggered earlier; they gathered behind the virtual fish for longer and displayed periods with reduced velocity and dispersion at each shoal passage than with parrotfish (Fig. 5e–h). In the Forced choice task, postlarval fish tended to prefer size-matched parrotfish rather than predators. Altogether, these findings provide evidence that, based on visual cues alone, postlarval fish can distinguish a conspecific from an equally small but nonaggressive fish species, and a predator from an equally large but nonaggressive fish species, suggesting that postlarval surgeonfish respond behaviourally not only to size but also to the shape and colour pattern of virtual fish.

Over the last two decades, a range of studies have demonstrated that postlarval fish possess well-developed behavioural and sensory abilities, rejecting the traditional paradigm that they are passive plankton (Beldade et al., 2012, 2016; Leis, 2015). In particular, postlarval fish survival depends on their ability to correctly evaluate sensory cues and select appropriate behavioural responses, for example to move towards conspecifics or flee predators (Barth et al., 2015). Among the sensory cues used by postlarval coral reef fish, visual cues are the most discussed, but their importance is the least understood (Lecchini et al., 2014). The visual abilities of postlarval fish increase during their pelagic life to reach a maximum near the onset of metamorphosis (Lara, 2001). Our experiments yielded convincing and quantified behavioural results highlighting the role of visual cues in postlarval fishes at a stage in their development during which they seek a suitable recruitment habitat. In particular, postlarval surgeonfish showed marked attraction towards corals, potentially due to the complex 3D structures with which they are associated. Furthermore, postlarval fish used visual cues to discriminate between conspecifics and predators and tailored their movement and behaviour to either follow their conspecifics (in ecological settings, this could be used to find a suitable settlement habitat) or avoid predation.

VR FOR BEHAVIOURAL STUDIES

Proof of Concept

The experimental study described above shows that postlarval coral reef convict surgeonfish visually recognize possible hiding places, adult conspecifics and bluefin jack predators, presented virtually. These results provide a successful proof of concept of our innovative virtual reality set-up with automated tracking of fish responses to simulated 3D models of habitats and fish shoals. We overcame two technical challenges: we simulated 3D models of fishes and habitats that were realistic enough to elicit natural reactions in postlarval coral reef fish, and we detected their individual positions in the aquarium in real time during the trials using a video-based tracking system. The detailed behavioural reactions of surgeonfish postlarvae to conspecifics and predators through several relevant kinematic measures such as their position in the aquarium, individual swimming speed and group dispersion and the multifactorial analysis of these measures enabled us to disentangle responses that could yield very similar results in less controlled experimental designs (sand versus corals, parrotfish versus bluefin jacks, butterflyfish versus surgeonfish).

Current Limitations and Solutions

In this project, we relied on the Microsoft Kinect Azure depth camera, an IR-based technology that proved unsuitable for underwater tracking, forcing us to use only its embedded colour camera. Tracking with a single camera limits the detection of fish in the aquarium to 2D horizontal positions, so we blocked the real-time updating of the viewpoint (see Video-based tracking section). Rendering of the animated scene was, however, geometrically correct at the centre, and distortions remained limited within the focal aquarium. We believe the behavioural response to the presentation of virtual coral reef habitats would be stronger with the real-time updating of the viewpoint, by enhancing the fish's sensation of physically reaching the virtual anfractuosities. To overcome these limitations in our future projects, we recently updated the VR set-up to include a pair of high-resolution colour cameras, and developed a complex underwater calibration procedure. Today, we can triangulate the detected fish positions from each view, to compute in real-time a fish's 3D position and update the rendering viewpoint in the virtual scene accordingly. Coupling tracking data with the simulation also allows us to place the desired test stimulus in the line of sight of focal individuals.

Perspectives

Numerous other simulations could be used with this experimental set-up to test a wide variety of parameters on coral reef fishes at different stages of development or test coral reef fishes reared in different conditions or exposed to different stresses prior to the visual cue experiment, and quantitatively characterize the impact on their behaviour. The use of VR offers countless new research opportunities including to better understand behaviours of coral reef fish in response to local and global changes (Beldade

et al., 2017; Mills et al., 2020; Nedelec et al., 2017; Schligler et al., 2021) and how they impact the role of vision in habitat selection at recruitment. To understand the mechanisms involved in the visual recognition of conspecifics or predators, our VR set-up can be used to manipulate as many visual factors as needed, including not only size, colour patterns and fin arrangements but also the behaviour of other individuals (aggressive, curious, social, fleeing). Even though some experimental protocols with real fish in aquaria partially control for these factors and facilitate observations compared to in situ protocols (e.g. Besson et al., 2017; Katzir, 1981; Roux et al., 2016), the acclimation time required to perform experiments limits the range of possible manipulations. In addition, when real fish are used as stimuli (e.g. Lecchini et al., 2014), the experiment cannot be reproduced multiple times in a reliably comparable manner, as the movement of the stimulus fish cannot be controlled. This study demonstrates that VR, even with a static rendering viewpoint, provides an excellent methodology to apply perfectly controlled virtual stimuli, which postlarval fish are able to correctly identify. VR can reproduce fairly realistic natural situations that can yield robust statistical results and allow for highly precise quantifications of postlarval behaviour in response to highly diverse scenarios. In addition, video-based modern tracking technologies have recently emerged in the field of animal behaviour and neuroscience, offering the possibility to conduct fine-grained kinematic analyses of the reactions of animals to specific situations (Barker & Baier, 2015; Drew, 2019; Dunn et al., 2016; Harpaz et al., 2021; Harvey et al., 2009; Larsch & Baier, 2018; Portugues & Engert, 2009; Stowers et al., 2017).

In conclusion, we have shown proof of concept of our new VR visual simulation set-up combined with an automated tracking system in an aquarium. There are, however, both benefits and disadvantages of studying fish behaviour with such technology. Benefits include shorter habituation phases in the aquarium (approximately 30 s compared to 5–7 min when experimenting with non-VR methods; see Nanninga et al., 2017), which we attributed to the nonaggressive immersive baseline environment; perfect control of the visual simulation (timing and content) allowing for the same simulations to be repeated within or between individuals several times; the possibility to test the same individuals in multiple successive trials, and in a controlled order; and, as mentioned earlier, the set-up enabled us to automatically collect numerous parameters about the kinematics of fish reactions in real-time, which contributed to a precise and objective characterization of their behaviour. Disadvantages include testing the behaviour of fish in a laboratory setting out of their natural milieu, with a visual rendering that cannot reach the quality of a real environment, and the technical skills in computer science required to prepare experiments and to process the large amount of data. However, this successful proof of concept of our new VR set-up and automated tracking system on relatively fragile and small postlarval coral reef fish in response to both habitats and different fish species holds significant promise for the field of fish behavioural ecology across all life stages and fish species in response to multiple biotic and abiotic conditions. The experimental VR set-up can be scaled up or down as a function of the size of the focal fish and, as such, it holds tremendous promise for the future of the study of teleost behaviour.

Author Contributions

Manuel Vidal: Conceptualization, Methodology, Software, Formal analysis, Investigation, Data curation, Writing–Original draft, Writing–Review & editing, Supervision. **Suzanne Mills:** Writing–Original draft, Writing–Review & editing. **Emma Gairin:** Writing–Original draft. **Frédéric Bertucci:** Writing–Original draft. **David Lecchini:** Conceptualization, Investigation, Resources, Writing–Original draft, Supervision, Funding acquisition.

Data Availability

Data files, global plots (all groups), and individual plots (trajectories, position scatter plots, animated position density maps, grouped bin data) and the Python code used for data processing for each experiment can be found in the following public repository: https://amubox.univ-amu.fr/s/WyYRBirn3pmzoqT.

Declaration of Interest

None.

Acknowledgments

We thank the technical staff of the CRIOBE for their support, and in particular Matthieu Reynaud for capturing the larvae used in the experiments. This work received support from the French government under the France 2030 investment plan, as part of the Initiative d'Excellence d'Aix-Marseille Université – A*MIDEX, from the Fondation de France (2019-08602), from the Office Français de la Biodiversité (AFB/2019/385 – OFB.20.0888) and from the Agence Nationale de la Recherche (ANR-19-CE34-0006-Manini and ANR-19-CE14-0010-SENSO) and from Université PSL (Global seed fund 2023 to SCM).

Supplementary Material

Supplementary material associated with this article is available, in the online version, at https://doi.org/10.1016/j.anbehav.2023.09.013.

References

Alatalo, R. V., Höglund, J., & Lundberg, A. (1991). Lekking in the black grouse. A test of male viability. *Nature, 352*(6331), 155–156.

Atema, J., Kingsford, M. J., & Gerlach, G. (2002). Larval reef fish could use odour for detection, retention and orientation to reefs. *Marine Ecology Progress Series, 241*, 151–160. https://doi.org/10.3354/meps241151

Baldauf, S. A., Kullmann, H., Thünken, T., Winter, S., & Bakker, T. C. M. (2009). Computer animation as a tool to study preferences in the cichlid *Pelvicachromis taeniatus*. *Journal of Fish Biology, 75*(3), 738–746. https://doi.org/10.1111/j.1095-8649.2009.02347.x

Barker, A. J., & Baier, H. (2015). Sensorimotor decision making in the zebrafish tectum. *Current Biology: CB, 25*(21), 2804–2814. https://doi.org/10.1016/j.cub.2015.09.055

Barth, P., Berenshtein, I., Besson, M., Roux, N., Parmentier, E., Banaigs, B., & Lecchini, D. (2015). From the ocean to a reef habitat: How do the larvae of coral reef fishes find their way home? A state of art on the latest advances. *Vie et Milieu, 65*(2), 91–100.

Beldade, R., Blandin, A., O'Donnell, R., & Mills, S. C. (2017). Cascading effects of thermally-induced anemone bleaching on associated anemonefish hormonal stress response and reproduction. *Nature Communications, 8*(1), 716. https://doi.org/10.1038/s41467-017-00565-w

Beldade, R., Holbrook, S. J., Schmitt, R. J., Planes, S., & Bernardi, G. (2016). Spatial patterns of self-recruitment of a coral reef fish in relation to island-scale retention mechanisms. *Molecular Ecology, 25*(20), 5203–5211.

Beldade, R., Holbrook, S. J., Schmitt, R. J., Planes, S., Malone, D., & Bernardi, G. (2012). Larger female fish contribute disproportionately more to self-replenishment. *Proceedings of the Royal Society B: Biological Sciences, 279*(1736), 2116–2121.

Besson, M., Feeney, W. E., Moniz, I., François, L., Brooker, R. M., Holzer, G., Metian, M., Roux, N., Laudet, V., & Lecchini, D. (2020). Anthropogenic stressors impact fish sensory development and survival via thyroid disruption. *Nature Communications, 11*(1), 3614. https://doi.org/10.1038/s41467-020-17450-8

Besson, M., Gache, C., Bertucci, F., Brooker, R. M., Roux, N., Jacob, H., Berthe, C., Sovrano, V. A., Dixson, D. L., & Lecchini, D. (2017). Exposure to agricultural pesticide impairs visual lateralization in a larval coral reef fish. *Scientific Reports, 7*(1). https://doi.org/10.1038/s41598-017-09381-0. Article 1.

Booth, D. J. (1992). Larval settlement patterns and preferences by domino damselfish *Dascyllus albisella* Gill. *Journal of Experimental Marine Biology and Ecology, 155*(1), 85–104.

Brookes, J., Warburton, M., Alghadier, M., Mon-Williams, M., & Mushtaq, F. (2020). Studying human behavior with virtual reality: The Unity Experiment

Framework. *Behavior Research Methods, 52*(2), 455–463. https://doi.org/10.3758/s13428-019-01242-0
Carmichael, L. (1952). [Review of the book *The study of instinct*, by N. Tinbergen]. *Science, 115*(2990), 438–439.
Coppock, A. G., Gardiner, N. M., & Jones, G. P. (2013). Olfactory discrimination in juvenile coral reef fishes: Response to conspecifics and corals. *Journal of Experimental Marine Biology and Ecology, 443*, 21–26. https://doi.org/10.1016/j.jembe.2013.02.026
Doherty, P. J. (2002). Variable replenishment and the dynamics of reef fish populations. In P. F. Sale (Ed.), *Coral reef fishes* (pp. 327–355). Academic Press. https://doi.org/10.1016/B978-012615185-5/50019-0.
Drew, L. (2019). The mouse in the video game. *Nature, 567*, 158. https://doi.org/10.1038/d41586-019-00791-w
Dunn, T. W., Gebhardt, C., Naumann, E. A., Riegler, C., Ahrens, M. B., Engert, F., & Del Bene, F. (2016). Neural circuits underlying visually evoked escapes in larval zebrafish. *Neuron, 89*(3), 613–628. https://doi.org/10.1016/j.neuron.2015.12.021
Harpaz, R., Nguyen, M. N., Bahl, A., & Engert, F. (2021). Precise visuomotor transformations underlying collective behavior in larval zebrafish. *Nature Communications, 12*(1). https://doi.org/10.1038/s41467-021-26748-0. Article 1.
Harvey, C. D., Collman, F., Dombeck, D. A., & Tank, D. W. (2009). Intracellular dynamics of hippocampal place cells during virtual navigation. *Nature, 461*(7266). https://doi.org/10.1038/nature08499. Article 7266.
Holles, S., Simpson, S. D., Radford, A. N., Berten, L., & Lecchini, D. (2013). Boat noise disrupts orientation behaviour in a coral reef fish. *Marine Ecology Progress Series, 485*, 295–300. https://doi.org/10.3354/meps10346
Holzer, G., Besson, M., Lambert, A., François, L., Barth, P., Gillet, B., Hughes, S., Piganeau, G., Leulier, F., Viriot, L., Lecchini, D., & Laudet, V. (2017). Fish larval recruitment to reefs is a thyroid hormone-mediated metamorphosis sensitive to the pesticide chlorpyrifos. *Elife, 6*, Article e27595. https://doi.org/10.7554/eLife.27595
Huang, K.-H., Rupprecht, P., Frank, T., Kawakami, K., Bouwmeester, T., & Friedrich, R. W. (2020). A virtual reality system to analyze neural activity and behavior in adult zebrafish. *Nature Methods, 17*(3). https://doi.org/10.1038/s41592-020-0759-2. Article 3.
Huijbers, C. M., Nagelkerken, I., Lössbroek, P. A. C., Schulten, I. E., Siegenthaler, A., Holderied, M. W., & Simpson, S. D. (2012). A test of the senses: Fish select novel habitats by responding to multiple cues. *Ecology, 93*(1), 46–55. https://doi.org/10.1890/10-2236.1
Ioannou, C. C., Guttal, V., & Couzin, I. D. (2012). Predatory fish select for coordinated collective motion in virtual prey. *Science, 337*(6099), 1212–1215. https://doi.org/10.1126/science.1218919
Katzir, G. (1981). Visual aspects of species recognition in the damselfish *Dascyllus aruanus* L. (Pisces, Pomacentridae). *Animal Behaviour, 29*(3), 842–849. https://doi.org/10.1016/S0003-3472(81)80019-X
Künzler, R., & Bakker, T. (1998). Computer animations as a tool in the study of mating preferences. *Behaviour, 135*(8), 1137–1159. https://doi.org/10.1163/156853998792913537
Lara, M. R. (2001). Morphology of the eye and visual acuities in the settlement-intervals of some Coral Reef Fishes (Labridae, Scaridae). *Environmental Biology of Fishes, 62*(4), 365–378. https://doi.org/10.1023/A:1012214229164
Larsch, J., & Baier, H. (2018). Biological motion as an innate perceptual mechanism driving social affiliation. *Current Biology, 28*(22), 3523–3532.e4. https://doi.org/10.1016/j.cub.2018.09.014
Lecchini, D., & Galzin, R. (2003). Influence of pelagic and benthic, biotic and abiotic, stochastic and deterministic processes on the dynamics of auto-recruitment of coral reef fish: A review. *Cybium, 27*, 167–184.
Lecchini, D., Peyrusse, K., Lanyon, R. G., & Lecellier, G. (2014). Importance of visual cues of conspecifics and predators during the habitat selection of coral reef fish larvae. *Comptes Rendus Biologies, 337*(5), 345–351. https://doi.org/10.1016/j.crvi.2014.03.007
Lecchini, D., Shima, J., Banaigs, B., & Galzin, R. (2005). Larval sensory abilities and mechanisms of habitat selection of a coral reef fish during settlement. *Oecologia, 143*(2), 326–334. https://doi.org/10.1007/s00442-004-1805-y
Lecchini, D., Waqalevu, V. P., Parmentier, E., Radford, C. A., & Banaigs, B. (2013). Fish larvae prefer coral over algal water cues: Implications of coral reef degradation. *Marine Ecology Progress Series, 475*, 303–307. https://doi.org/10.3354/meps10094
Leis, J. M. (2015). Is dispersal of larval reef fishes passive? In C. Mora (Ed.), *Ecology of fishes on coral reefs* (pp. 223–226). Cambridge University Press.
Leis, J. M., & Carson-Ewart, B. M. (1999). In situ swimming and settlement behaviour of larvae of an Indo-Pacific coral-reef fish, the coral trout *Plectropomus leopardus* (Pisces: Serranidae). *Marine Biology, 134*(1), 51–64. https://doi.org/10.1007/s002270050524
Leis, J. M., & McCormick, M. I. (2002). The biology, behavior, and ecology of the pelagic, larval stage of coral reef fishes. In P. F. Sale (Ed.), *Coral reef fishes* (pp. 171–199). Academic Press. https://doi.org/10.1016/B978-012615185-5/50011-6.
Losey, G. S., McFarland, W. N., Loew, E. R., Zamzow, J. P., Nelson, P. A., & Marshall, N. J. (2003). Visual biology of Hawaiian coral reef fishes. I. Ocular transmission and visual pigments. *Copeia, 2003*(3), 433–454.
McCormick, M. I., Makey, L., & Dufour, V. (2002). Comparative study of metamorphosis in tropical reef fishes. *Marine Biology, 141*(5), 841–853.
Mills, S. C., Alatalo, R. V., Koskela, E., Mappes, J., Mappes, T., & Oksanen, T. A. (2007). Signal reliability compromised by genotype-by-environment interaction and potential mechanisms for its preservation. *Evolution; International Journal of Organic Evolution, 61*(7), 1748–1757. https://doi.org/10.1111/j.1558-5646.2007.00145.x
Mills, S. C., Beldade, R., Henry, L., Laverty, D., Nedelec, S. L., Simpson, S. D., & Radford, A. N. (2020). Hormonal and behavioural effects of motorboat noise on wild coral reef fish. *Environmental Pollution, 262*, Article 114250. https://doi.org/10.1016/j.envpol.2020.114250
Montgomery, J. C., Jeffs, A., Simpson, S. D., Meekan, M., & Tindle, C. (2006). Sound as an orientation cue for the pelagic larvae of reef fishes and decapod crustaceans. *Advances in Marine Biology, 51*, 143–196. https://doi.org/10.1016/S0065-2881(06)51003-X
Mossio, M., Vidal, M., & Berthoz, A. (2008). Traveled distances: New insights into the role of optic flow. *Vision Research, 48*(2), 289–303.
Myrberg, A. A., & Fuiman, L. A. (2002). The sensory world of coral reef fishes. In P. F. Sale (Ed.), *Coral reef fishes: Dynamics and diversity in a complex ecosystem* (pp. 123–148). Academic Press.
Nanninga, G. B., Côté, I. M., Beldade, R., & Mills, S. C. (2017). Behavioural acclimation to cameras and observers in coral reef fishes. *Ethology, 123*(10), 705–711. https://doi.org/10.1111/eth.12642
Nedelec, S. L., Mills, S. C., Radford, A. N., Beldade, R., Simpson, S. D., Nedelec, B., & Côté, I. M. (2017). Motorboat noise disrupts co-operative interspecific interactions. *Scientific Reports, 7*(1), 6987. https://doi.org/10.1038/s41598-017-06515-2
Neri, P. (2012). Feature binding in zebrafish. *Animal Behaviour, 84*(2), 485–493. https://doi.org/10.1016/j.anbehav.2012.06.005
Parmentier, E., Berten, L., Rigo, P., Aubrun, F., Nedelec, S. L., Simpson, S. D., & Lecchini, D. (2015). The influence of various reef sounds on coral-fish larvae behaviour. *Journal of Fish Biology, 86*(5), 1507–1518. https://doi.org/10.1111/jfb.12651
Portugues, R., & Engert, F. (2009). The neural basis of visual behaviors in the larval zebrafish. *Current Opinion in Neurobiology, 19*(6), 644–647. https://doi.org/10.1016/j.conb.2009.10.007
Rosenthal, G. G., & Evans, C. S. (1998). Female preference for swords in *Xiphophorus helleri* reflects a bias for large apparent size. *Proceedings of the National Academy of Sciences of the United States of America, 95*(8), 4431–4436. https://doi.org/10.1073/pnas.95.8.4431
Roux, N., Duran, E., Lanyon, R. G., Frédérich, B., Berthe, C., Besson, M., Dixson, D. L., & Lecchini, D. (2016). Brain lateralization involved in visual recognition of conspecifics in coral reef fish at recruitment. *Animal Behaviour, 117*, 3–8. https://doi.org/10.1016/j.anbehav.2016.04.011
Saverino, C., & Gerlai, R. (2008). The social zebrafish: Behavioral responses to conspecific, heterospecific, and computer animated fish. *Behavioural Brain Research, 191*(1), 77–87. https://doi.org/10.1016/j.bbr.2008.03.013
Schligler, J., Cortese, D., Beldade, R., Swearer, S. E., & Mills, S. C. (2021). Long-term exposure to artificial light at night in the wild decreases survival and growth of a coral reef fish. *Proceedings of the Royal Society B: Biological Sciences, 288*(1952), Article 20210454. https://doi.org/10.1098/rspb.2021.0454
Siu, G., Bacchet, P., Bernardi, G., Brooks, A. J., Carlot, J., Causse, R., Claudet, J., Clua, É., Delrieu-Trottin, E., Espiau, B., Harmelin-Vivien, M., Keith, P., Lecchini, D., Madi-Moussa, R., Parravicini, V., Planes, S., Ponsonnet, C., Randall, J. E., Sasal, P., & Galzin, R. (2017). Shore fishes of French Polynesia. *Cybium, 41*(3), 245–278.
Stowers, J. R., Hofbauer, M., Bastien, R., Griessner, J., Higgins, P., Farooqui, S., Fischer, R. M., Nowikovsky, K., Haubensak, W., Couzin, I. D., Tessmar-Raible, K., & Straw, A. D. (2017). Virtual reality for freely moving animals. *Nature Methods, 14*(10), 995–1002. https://doi.org/10.1038/nmeth.4399
Tarr, M. J., & Warren, W. H. (2002). Virtual reality in behavioral neuroscience and beyond. *Nature Neuroscience, 5*(Suppl), 1089–1092.
Tettamanti, V., de Busserolles, F., Lecchini, D., Marshall, N. J., & Cortesi, F. (2019). Visual system development of the spotted unicornfish, *Naso brevirostris* (Acanthuridae). *Journal of Experimental Biology, 222*(24), Article 209916. https://doi.org/10.1242/jeb.209916
Tolimieri, N., Haine, O., Jeffs, A., McCauley, R., & Montgomery, J. (2004). Directional orientation of pomacentrid larvae to ambient reef sound. *Coral Reefs, 23*(2), 184–191. https://doi.org/10.1007/s00338-004-0383-0
Vail, A. L., & McCormick, M. I. (2011). Metamorphosing reef fishes avoid predator scent when choosing a home. *Biology Letters, 7*(6), 921–924. https://doi.org/10.1098/rsbl.2011.0380
Vidal, M., Amorim, M.-A., & Berthoz, A. (2004). Navigating in a virtual three-dimensional maze: How do egocentric and allocentric reference frames interact? *Cognitive Brain Research, 19*(3), 244–258.
Vidal, M., & Bülthoff, H. H. (2009). Storing upright turns: How visual and vestibular cues interact during the encoding and recalling process. *Experimental Brain Research, 200*(1), 37–49. https://doi.org/10.1007/s00221-009-1980-5
Vidal, M., Lehmann, A., & Bülthoff, H. H. (2009). A multisensory approach to spatial updating: The case of mental rotations. *Experimental Brain Research, 197*(1), 59–68. https://doi.org/10.1007/s00221-009-1892-4

Appendix

Table A1
Experiment 1's best behavioural model fitting

Habitat effect				Species effect			
Condition	Best model	Parameters	RMSE	Condition	Best model	Parameters	RMSE
X-position							
Sand control	**Quadratic**	***a*=−0.004, *b*=0.489, *c*=−3.445**	**5.59**	Conspecific	**Quadratic**	***a*=0.008, *b*=−0.581, *c*=4.006**	**11.42**
Healthy coral	**Linear**	***a*=−0.132, *b*=9.209**	**9.13**	Predator	Exponential	*s*=−3.506, *l*=−45.064, *k*=0.172	3.93
Bleached coral	**Quadratic**	***a*=0.005, *b*=−0.389, *c*=14.843**	**8.51**	Neutral	**Quadratic**	***a*=−0.007, *b*=0.627, *c*=−6.574**	**7.40**
Y-position							
Sand control	**Linear**	***a*=0.081, *b*=12.659**	**4.78**	Conspecific	Quadratic	*a*=−0.007, *b*=0.881, *c*=−18.470	7.41
Healthy coral	**Quadratic**	***a*=−0.008, *b*=0.627, *c*=1.228**	**7.99**	Predator	Linear	*a*=0.238, *b*=5.842	4.57
Bleached coral	**Exponential**	***s*=33.413, *l*=5.127, *k*=0.142**	**6.84**	Neutral	**Linear**	***a*=0.025, *b*=3.738**	**7.20**
Velocity							
Sand control	**Linear**	***a*=0.025, *b*=13.637**	**2.66**	Conspecific	**Quadratic**	***a*=−0.002, *b*=0.252, *c*=16.156**	**3.78**
Healthy coral	**Linear**	***a*=0.016, *b*=23.210**	**3.24**	Predator	Exponential	*s*=42.560, *l*=6.096, *k*=0.301	1.94
Bleached coral	**Exponential**	***s*=15.511, *l*=24.201, *k*=0.203**	**2.88**	Neutral	Linear	*a*=0.095, *b*=14.962	2.77
Dispersion							
Sand control	**Exponential**	***s*=46.648, *l*=38.060, *k*=0.080**	**3.01**	Conspecific	**Quadratic**	***a*=−0.002, *b*=0.212, *c*=41.197**	**3.91**
Healthy coral	**Quadratic**	***a*=−0.002, *b*=0.173, *c*=42.461**	**3.33**	Predator	Linear	*a*=−0.117, *b*=40.813	1.72
Bleached coral	**Exponential**	***s*=31.970, *l*=44.103, *k*=0.217**	**3.90**	Neutral	**Linear**	***a*=0.047, *b*=36.909**	**3.02**

The best model, parameters and corrected RMSE for each of the six conditions and four behavioural measures. See Table 1 for descriptions of parameters. For each fit, we assessed the quality of fits computing an RMSE distribution d_{RMSE} by fitting 1000 times data with shuffled time bins. Two quality criteria were used: RMSE < $P_{1\%}(d_{RMSE})$ and RMSE + 20% < mean(d_{RMSE}). Fits highlighted in bold did not meet the quality criteria.

Table A2
Experiment 2's best behavioural model fitting

Conspecific effect				Predator effect			
Condition	Best model	Parameters	RMSE	Condition	Best model	Parameters	RMSE
X-position							
Conspecific static	Quadratic	*a*=0.005, *b*=−0.492, *c*=−0.336	4.94	Predator static	Quadratic	*a*=0.006, *b*=−0.957, *c*=−4.335	2.42
Conspecific	Linear periodic	*a*=−0.131, *b*=17.240	7.05	Predator	Exponential periodic	*s*=22.873, *l*=6.347, *k*=0.057	4.37
1 pass		*A*=21.585, t_0=16.803		1 pass		*A*=9.486, t_0=12.677	
Conspecific	Linear periodic	*a*=0.020, *b*=17.755	5.20	Predator	Linear periodic	*a*=−0.404, *b*=19.353	3.93
3 pass		*A*=24.675, t_0=17.632		3 passes		*A*=14.600, t_0=12.759	
Y-position							
Conspecific static	**Exponential**	***s*=24.604, *l*=8.093, *k*=0.159**	**6.57**	Predator static	Quadratic	*a*=−0.009, *b*=0.792, *c*=18.338	5.00
Conspecific	Linear periodic	*a*=−0.399, *b*=34.457	7.08	Predator	Quadratic periodic	*a*=−0.006, *b*=0.515, *c*=21.644	3.88
1 pass		*A*=8.487, t_0=15.584		1 pass		*A*=4.745, t_0=19.068	
Conspecific	Exponential periodic	*s*=44.447, *l*=7.666, *k*=0.177	6.63	Predator	Exponential periodic	*s*=4.602, *l*=36.519, *k*=0.060	3.00
3 passes		*A*=41.769, t_0=13.242		3 passes		*A*=3.954, t_0=7.442	
Velocity							
Conspecific static	Linear	*a*=0.064, *b*=12.814	2.79	Predator static	Exponential	*s*=21.299, *l*=8.257, *k*=0.497	1.56
Conspecific	**Linear periodic**	***a*=−0.015, *b*=19.439**	**2.51**	Predator	Linear periodic	*a*=0.073, *b*=10.845	1.98
1 pass		***A*=1.408, t_0=3.883**		1 pass		*A*=1.505, t_0=5.195	
Conspecific	**Quadratic periodic**	***a*=−0.002, *b*=0.115, *c*=19.511**	**2.53**	Predator	Exponential periodic	*s*=19.405, *l*=12.386, *k*=0.269	2.00
3 passes		***A*=2.994, t_0=24.143**		3 passes		*A*=2.605, t_0=6.476	
Dispersion							
Conspecific static	**Linear**	***a*=0.036, *b*=38.272**	**2.90**	Predator static	Quadratic	*a*=−0.001, *b*=0.038, *c*=40.885	1.63
Conspecific	**Linear periodic**	***a*=−0.011, *b*=46.519**	**2.66**	Predator	Quadratic periodic	*a*=0.005, *b*=−0.350, *c*=37.443	3.20
1 pass		***A*=4.066, t_0=13.918**		1 pass		*A*=4.225, t_0=4.374	
Conspecific	**Linear periodic**	***a*=−0.003, *b*=47.685**	**3.22**	Predator	Exponential periodic	*s*=45.052, *l*=34.639, *k*=0.064	2.34
3 passes		***A*=3.742, t_0=1.631**		3 passes		*A*=2.560, t_0=7.751	

The best model, parameters and corrected RMSE for each of the six conditions and four behavioural measures. See Table 1 for descriptions of parameters. For each fit, we assessed the quality of fits computing an RMSE distribution d_{RMSE} by fitting 1000 times data with shuffled time bins. Two quality criteria were used: RMSE < $P_{1\%}(d_{RMSE})$ and RMSE + 20% < mean(d_{RMSE}). Fits highlighted in bold did not meet the quality criteria.

Table A3
Experiment 3's best behavioural model fitting

Conspecific effect				Predator effect			
Condition	Best model	Parameters	RMSE	Condition	Best model	Parameters	RMSE
X-position							
Conspecific	Linear periodic	a=0.808, b=−4.566 A=45.705, t_0=31.038	4.26	Predator	Linear periodic	a=0.019, b=18.456 A=36.905, t_0=29.70	2.41
Control	Linear periodic	a=0.407, b=3.059 A=26.336, t_0=24.652	4.29	Control	Exponential periodic	s=100.000, l=4.182, k=0.148 A=41.616, t_0=32.021	5.36
Forced choice	Linear periodic	a=−0.916, b=36.477 A=32.652, t_0=37.918	3.88	Forced choice	Linear periodic	a=0.292, b=−19.370 A=25.090, t_0=23.687	6.54
Y-position							
Conspecific	Linear periodic	a=0.445, b=−10.035 A=26.122, t_0=25.612	8.80	Predator	Quadratic periodic	a=0.026, b=−1.000, c=29.847 A=38.855, t_0=26.059	4.29
Control	Linear periodic	a=0.426, b=9.874 A=45.511, t_0=26.100	5.88	Control	Linear periodic	a=0.128, b=13.793 A=26.441, t_0=29.359	4.01
Forced choice	Linear periodic	a=0.099, b=11.310 A=28.637, t_0=29.114	5.47	Forced choice	Linear periodic	a=0.633, b=−1.310 A=24.457, t_0=24.211	4.36
Velocity							
Conspecific	**Exponential periodic**	**s=−100.0, l=30.610, k=0.248 A=4.612, t_0=12.036**	**2.60**	Predator	Quadratic periodic	a=0.015, b=−1.000, c=33.344 A=5.168, t_0=44.622	1.95
Control	**Quadratic periodic**	**a=0.016, b=−1.000, c=39.365 A=2.622, t_0=30.696**	**2.30**	Control	Linear periodic	a=−0.091, b=23.697 A=9.245, t_0=42.826	2.12
Forced choice	Linear periodic	a=0.117, b=24.698 A=3.597, t_0=7.308	2.25	Forced choice	Quadratic periodic	a=0.016, b=−1.000, c=36.671 A=1.504, t_0=45.773	1.87
Dispersion							
Conspecific	Linear periodic	a=−0.039, b=53.221 A=6.593, t_0=14.649	2.35	Predator	Quadratic periodic	a=−0.015, b=1.000, c=31.155 A=18.497, t_0=15.493	2.27
Control	Linear periodic	a=0.020, b=48.171 A=12.158, t_0=9.195	2.80	Control	Quadratic periodic	a=0.012, b=−1.000, c=65.723 A=7.195, t_0=11.917	1.90
Forced choice	Linear periodic	a=0.085, b=49.016 A=7.441, t_0=22.130	2.61	Forced choice	Linear periodic	a=−0.123, b=51.698 A=11.812, t_0=19.777	2.54

The best model, parameters and corrected RMSE for each of the six conditions and four behavioural measures. See Table 1 for descriptions of parameters. For each fit, we assessed the quality of fits computing an RMSE distribution d_{RMSE} by fitting 1000 times data with shuffled time bins. Two quality criteria were used: RMSE < $P_{1\%}(d_{RMSE})$ and RMSE + 20% < mean(d_{RMSE}). Fits highlighted in bold did not meet the quality criteria.

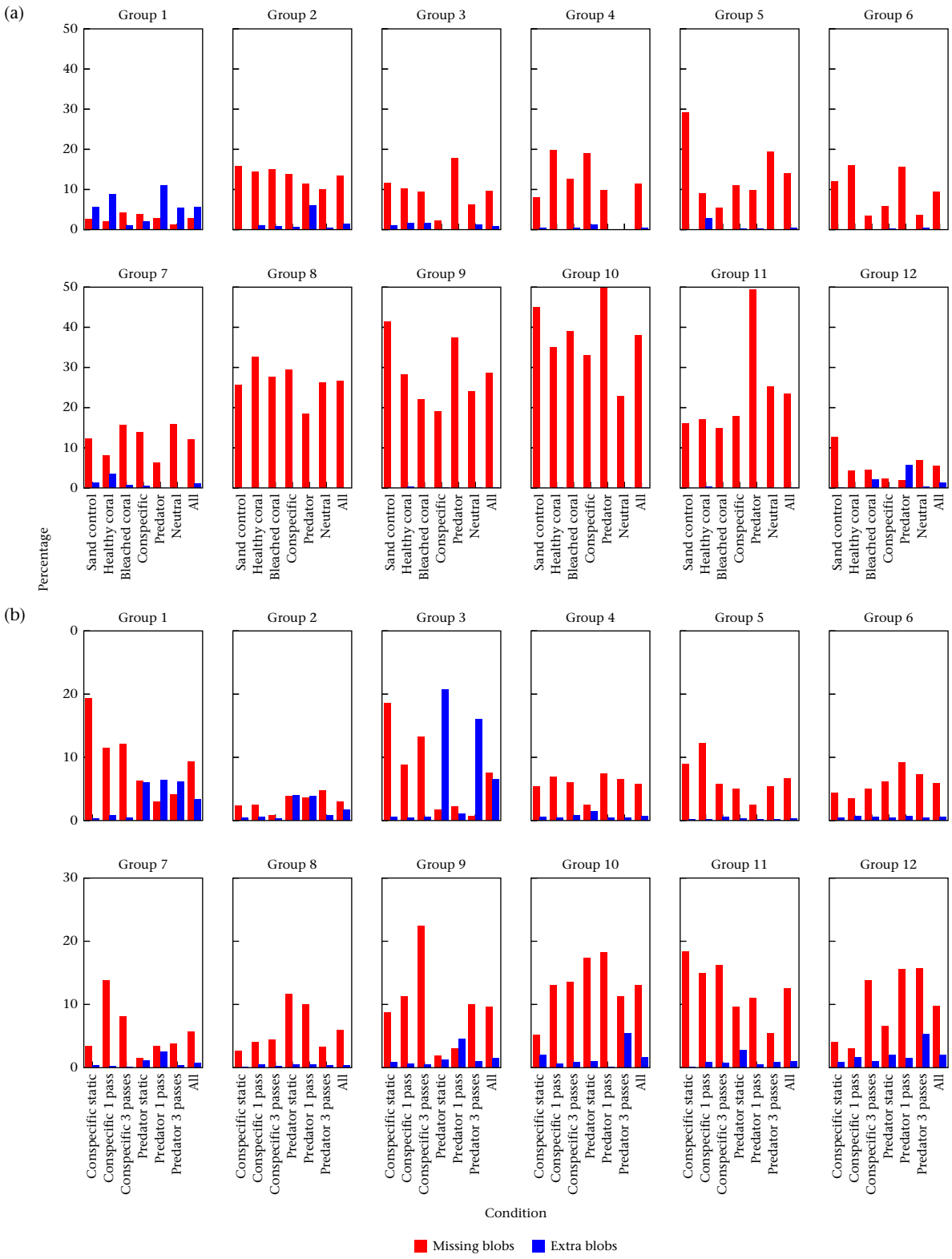

Figure A1. (a–c) Tracking performance for experiments 1–3. For each tested fish group and each condition, the average percentages of missing/extra blobs (i.e. detected fish locations) are given in red/blue. FC: forced choice. Tracking accuracy was evaluated by computing the average percentage of detected blobs relative to the number of expected blobs (five per frame) across all recorded frames of the trial. In experiment 1, on average, 16.3% of blobs were missing and 1.0% of extra blobs were detected. The tracking was rather poor for four groups (8, 9, 10 and 11), for which there were on average 29.3% missing blobs. However, these groups remained in the analyses as the sampling rate of 5 Hz was high enough for the overall data to be valid. To improve the tracking performance, we reduced the luminosity variation by using opaque black curtains for the experimental room's windows. In experiments 2 and 3, 8.9% and 10.9% of blobs were missing, and 1.5% and 1.3% of extra blobs were detected on average, respectively.

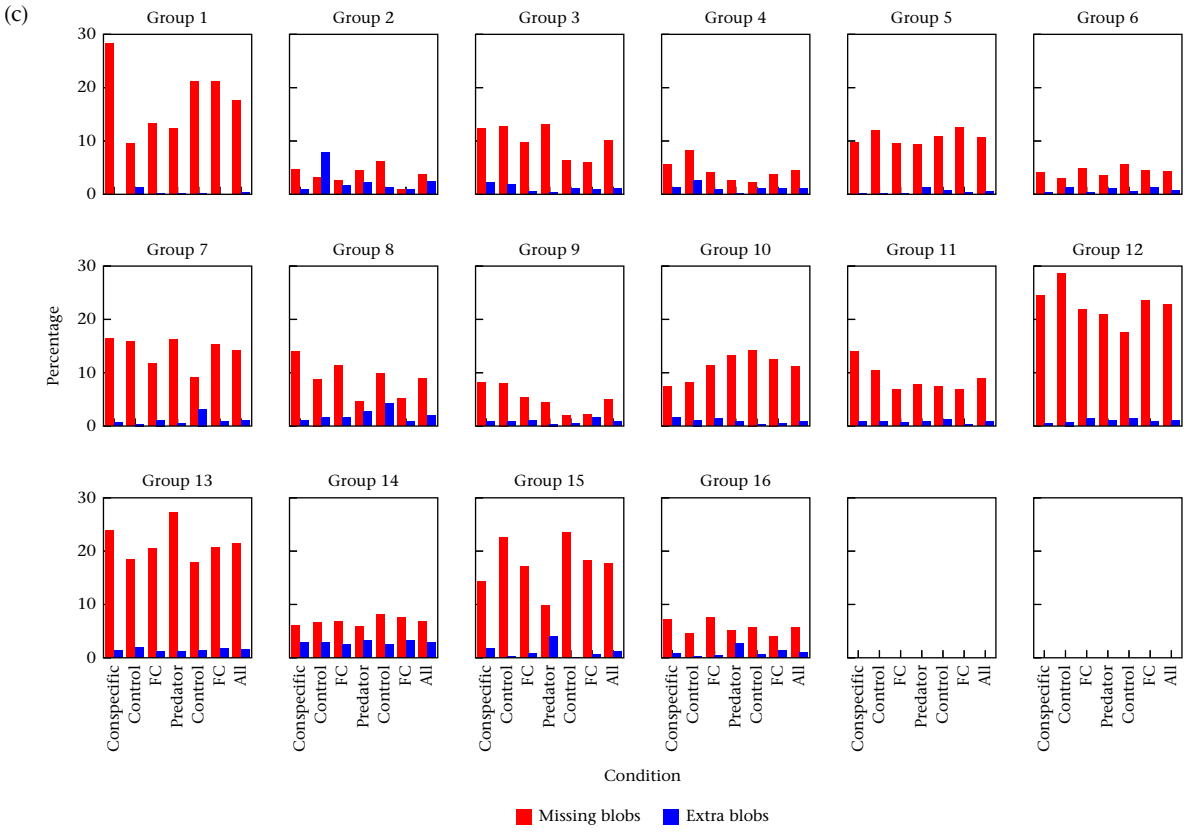

Figure A1. (*continued*).

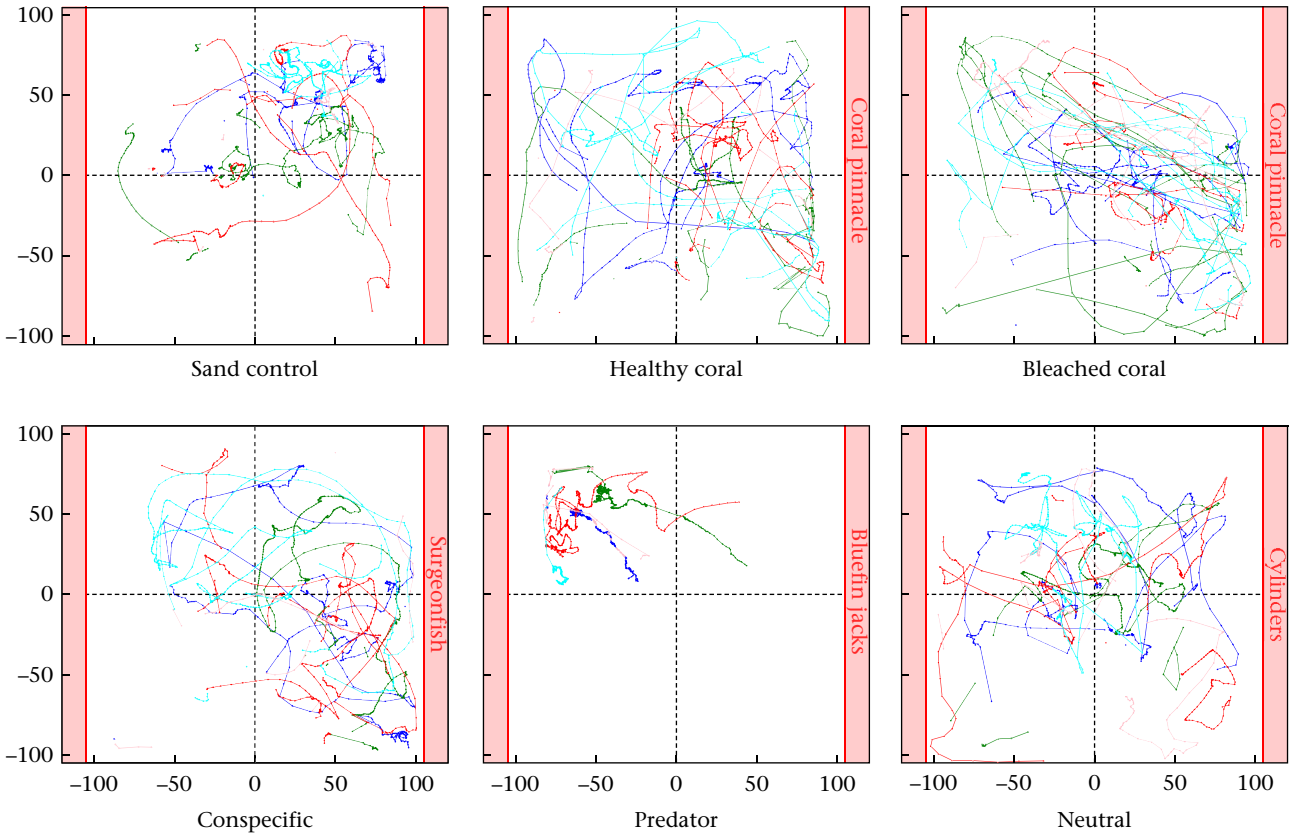

Figure A2. Example of individual trajectories reconstruction in experiment 1. Individual fish trajectories illustrating behavioural reactions of a typical group to the six stimuli presented on the aquarium sides (red shaded areas) in experiment 1 are shown. The validated positions of fish are connected by coloured lines using a minimal distance heuristic to track individual fish in successive frames.

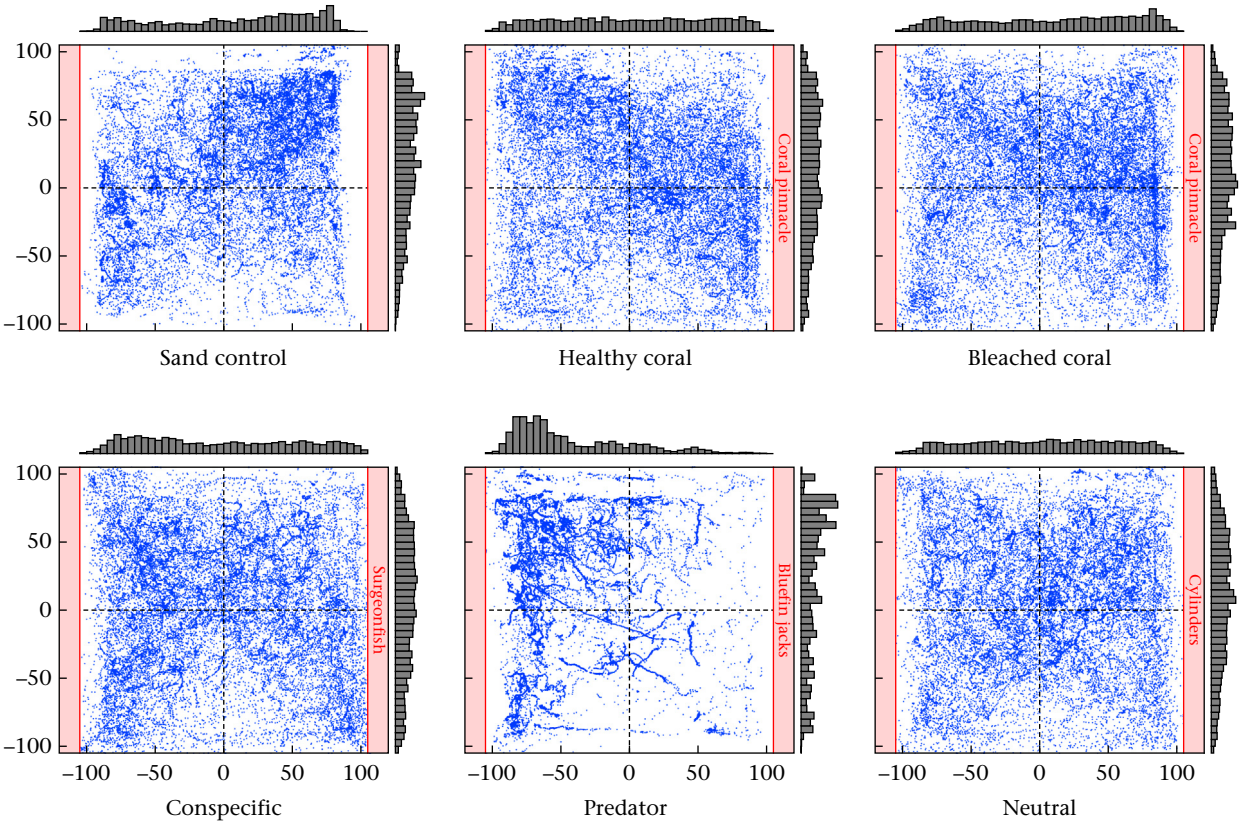

Figure A3. Experiment 1 raw results visualization. The 2D positions of all fish and all groups ($N = 12$) are shown for the six tested conditions: Sand control, Healthy coral, Bleached coral, Conspecific, Predator and Neutral. For each condition, the stimulus was presented on the right side. All valid positions detected at each frame throughout trial durations are presented. Normalized X- and Y-position distribution histograms are provided above and to the right of each plot.

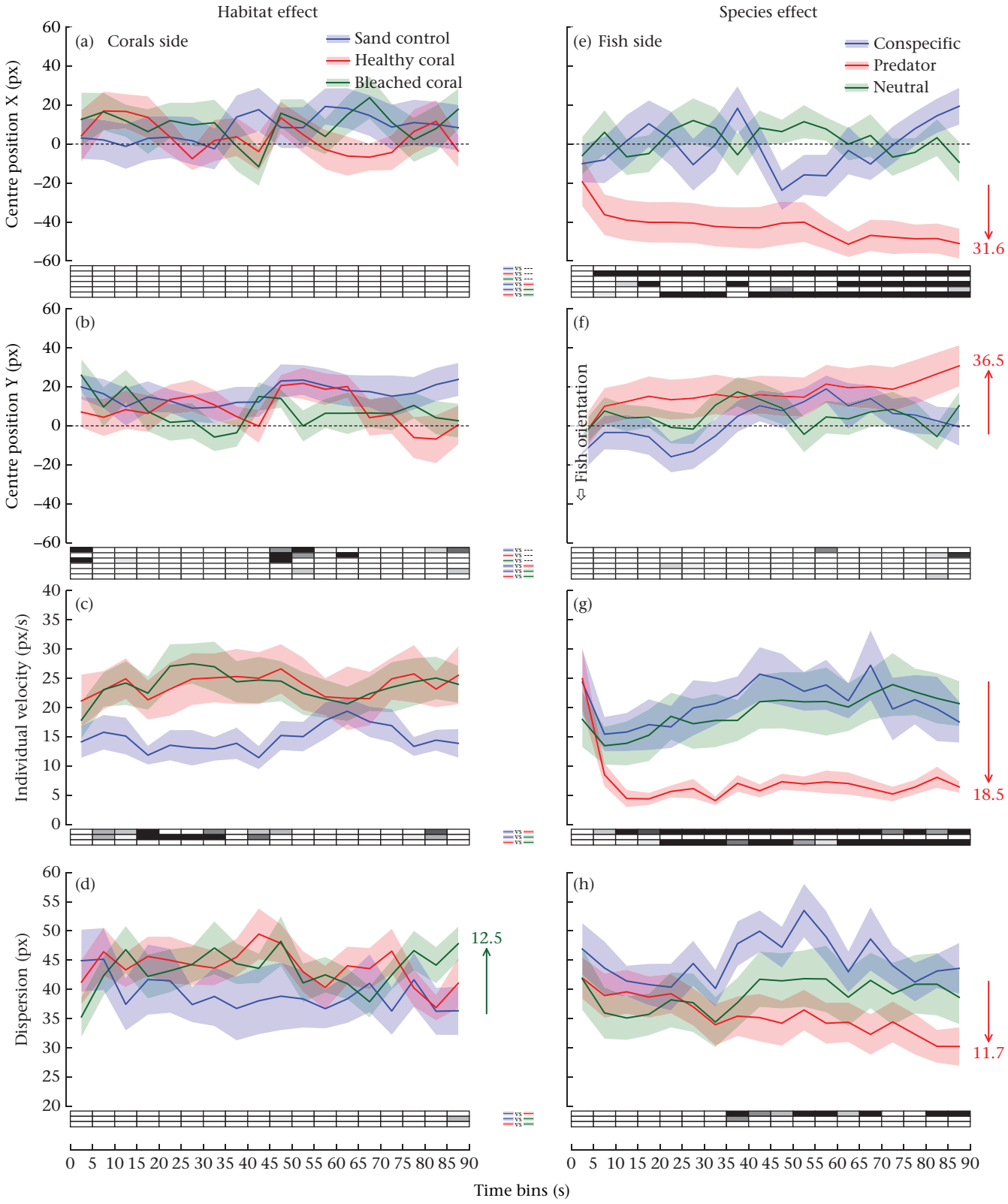

Figure A4. Experiment 1 group time series and statistics. The X- and Y-positions of the group centre, individual velocity and group dispersion are plotted in time bins of 5 s for the (a–d) Habitat effect and (e–h) Species effect. For each 5 s time bin, average performance in the conditions was compared to each other or to zero with paired and single-value Student *t* tests. Significance level is provided in the boxes below the plots (ranging from light grey for $P < 0.05/1$ to black for $P < 0.05/N_{Tests}$ using Bonferroni's correction for $N_{Tests} = 3$; white for $P > 0.05$).

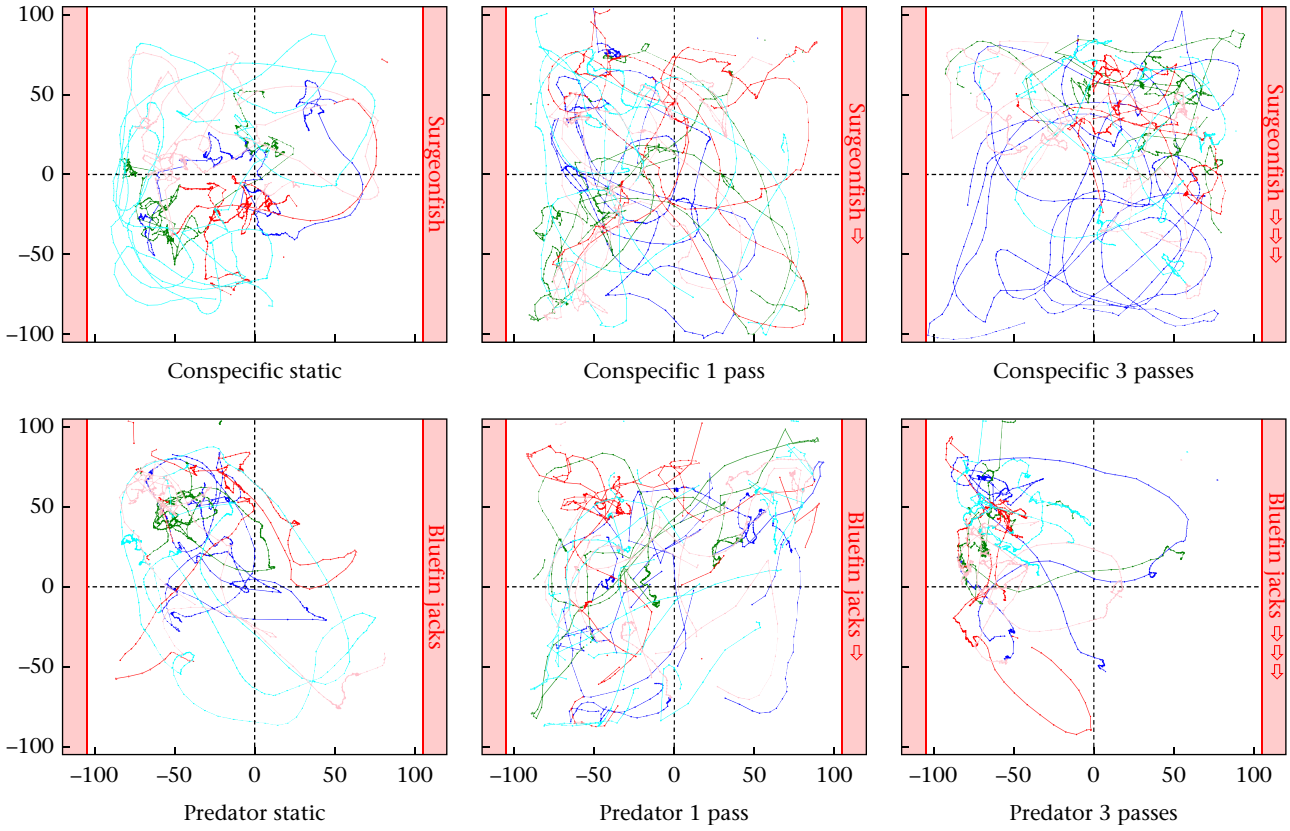

Figure A5. Example of individual trajectories reconstruction in experiment 2. Individual fish trajectories illustrating behavioural reactions of a typical group to the eight stimuli presented on the aquarium sides (red shaded areas) of experiment 2 are shown. The validated positions of fish are connected by coloured lines using a minimal distance heuristic to track individual fish in successive frames.

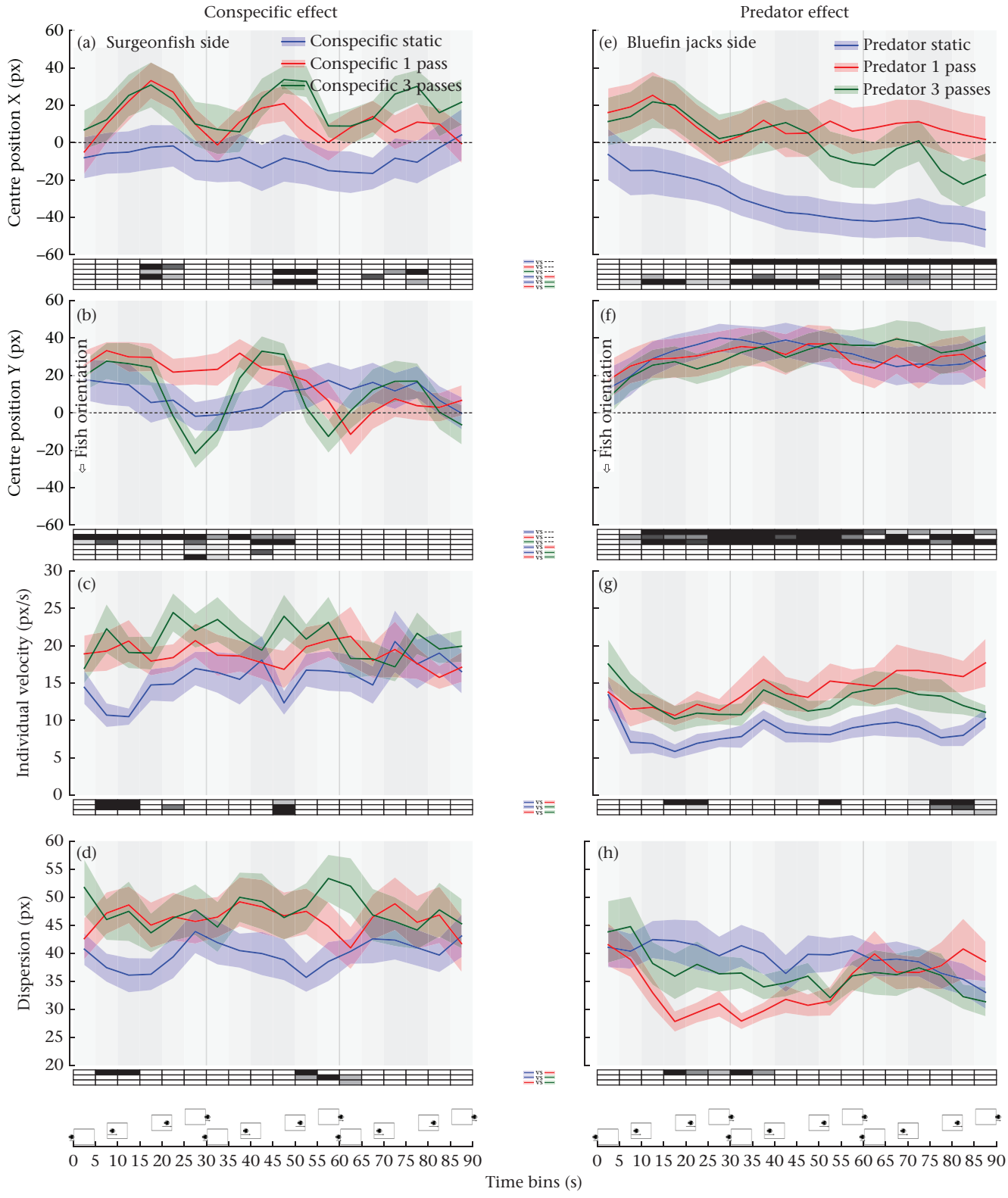

Figure A6. Experiment 2 group time series and statistics. The X- and Y-positions of the group centre, individual velocity and group dispersion are plotted in time bins of 5 s for the (a–d) Conspecific effect and (e–h) Predator effect. For each 5 s time bin, average performance in the conditions was compared to each other or to zero with paired and single-value Student *t* tests. Significance level is provided in the boxes below the plots (ranging from light grey for $P < 0.05/1$ to black for $P < 0.05/N_{Tests}$ using Bonferroni's correction for $N_{Tests} = 3$; white for $P > 0.05$). Shaded areas highlight the stimuli-critical periods based on the ongoing distance of the passing virtual shoals in the three-passes conditions (30 s periodicity) illustrated by the fish positions relative to the side screen shown above the time axis.

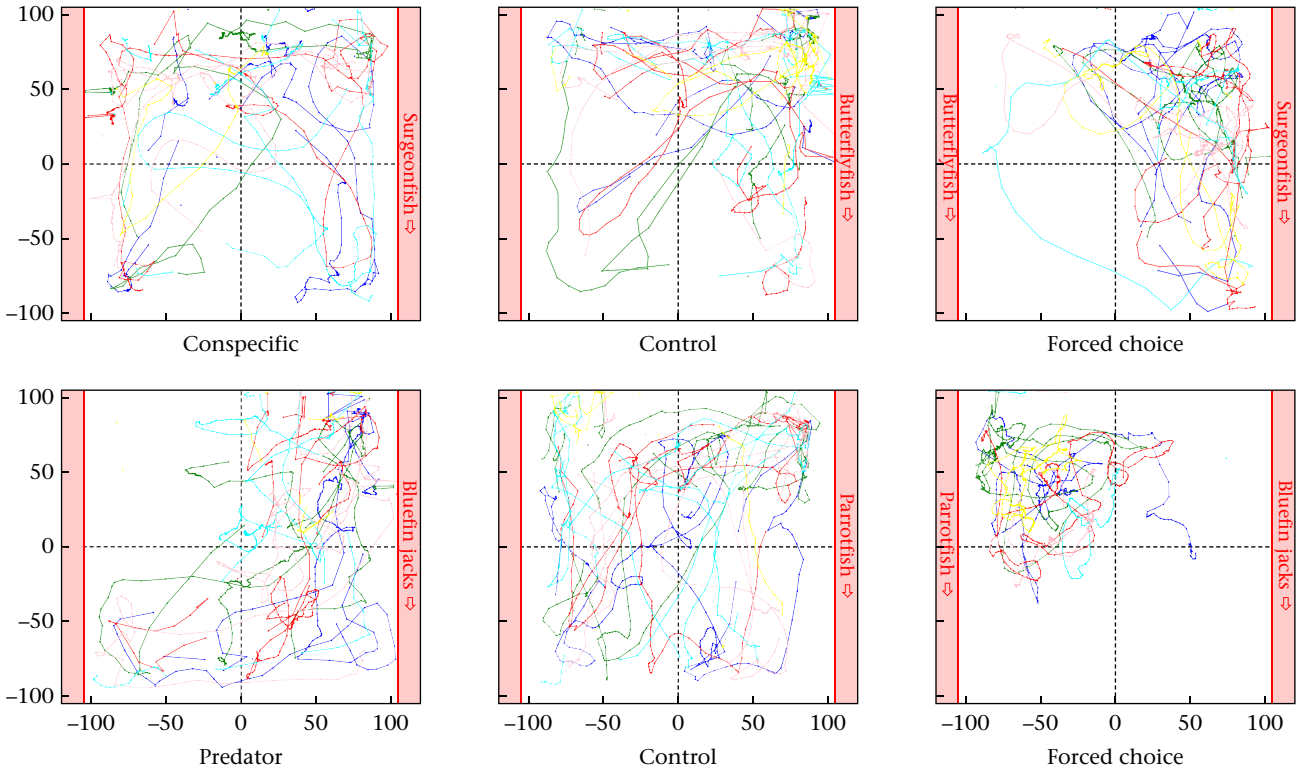

Figure A7. Example of individual trajectories reconstruction in experiment 3. Individual fish trajectories illustrating behavioural reactions of a typical group to the six stimuli presented on the aquarium sides (red shaded areas) of experiment 3 are shown. The validated positions of fish are connected by coloured lines using a minimal distance heuristic to track individual fish in successive frames.

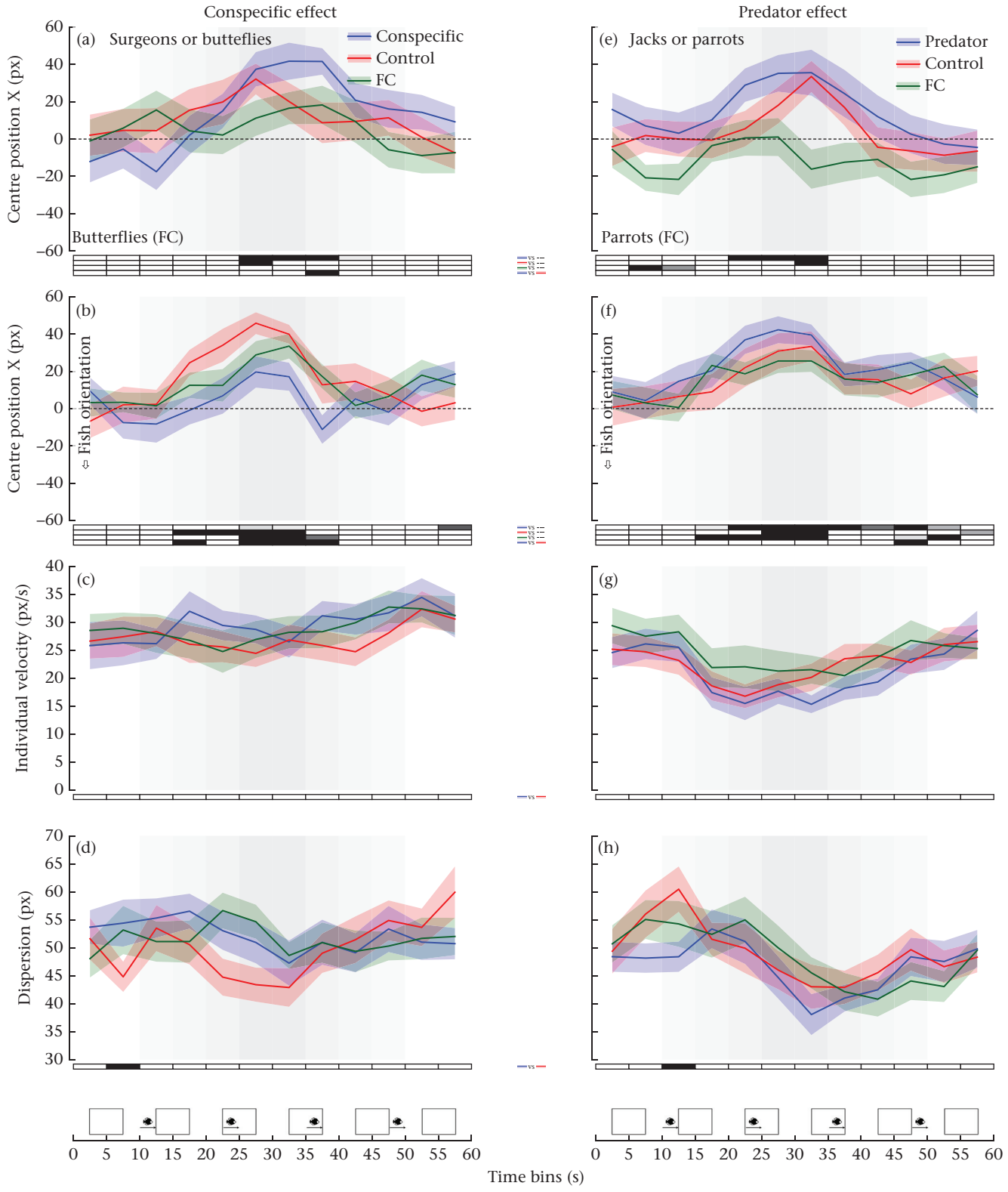

Figure A8. Experiment 3 group time series and statistics. The X- and Y-positions of the group centre, individual velocity and group dispersion are plotted in time bins of 5 s for the (a–d) Conspecific effect and (e–h) Predator effect. FC: forced choice. For each 5 s time bin, average performance in the conditions was compared to each other or to zero with paired and single-value Student *t* tests. Significance level is provided in the boxes below the plots (ranging from light grey for $P < 0.05/1$ to black for $P < 0.05/N_{Tests}$ using Bonferroni's correction for $N_{Tests} = 3$; white for $P > 0.05$). Shaded areas highlight the stimuli-critical period based on the ongoing distance of the passing virtual shoals illustrated by the fish positions relative to the side screen shown above the time axis.